Available online at www.sciencedirect.com
ScienceDirect
Coordination Chemistry Reviews 251 (2007) 2452–2476
COORDINATION CHEMISTRY REVIEWS
www.elsevier.com/locate/ccr

Review

Advances in the chemistry of carboranes and metallacarboranes with more than 12 vertices

Liang Deng, Zuowei Xie *

Department of Chemistry, The Chinese University of Hong Kong, Shatin, New Territories, Hong Kong, China

Received 12 October 2006; accepted 11 February 2007
Available online 15 February 2007

Contents

Abstract

Boron clusters with more than 12 vertices showing a very rich and diverse chemistry were confined to the 13- and 14-vertex metallacarboranes until 2003. Very recently, significant progress in the syntheses of 13- and 14-vertex carboranes has been made, leading to the preparation of 15-vertex metallacarboranes. These studies open up new possibilities for the development of polyhedral clusters of extraordinary size. This review summarizes the advances in this growing research field since the successful preparation of the first 13-vertex metallacarborane. Achievements, problems and perspectives are discussed in this article.

Keywords: Carborane; Metallacarborane; Lanthanide; *p*-Block metal; Supercarborane; Transition metal

1. Introduction

The chemistry of carboranes and metallacarboranes has received considerable attention since their emergence in the 1960s [1,2]. Efforts of almost half a century in this area have resulted in the extensive studies on the synthesis, structure, reactivity, and application of these clusters [3–21]. Progress in this field has been discussed in a number of reviews [8–21] and monographs [3–7]. This review will focus specifically on the advances in the chemistry of carboranes and metallacarboranes with more than 12 vertices. When the cluster size is concerned, icosahedral and sub-icosahedral carboranes dominate the research activities in the past five decades [3–21], and carboranes with more than 12 vertices (so called supercarbo-

* Corresponding author. Tel.: +852 26096269; fax: +852 26035057.
E-mail address: zxie@cuhk.edu.hk (Z. Xie).

0010-8545/$ – see front matter © 2007 Elsevier B.V. All rights reserved.
doi:10.1016/j.ccr.2007.02.009

ranes) were not known before 2003 [22]. It is only in recent years that significant progress been made in the chemistry of supercarboranes [23,24]. Subsequently, 15-vertex metallacarboranes were also prepared in 2006 [25,26]. These new achievements will be included in this review.

If no atom is indicated in the polyhedral structures shown in the following schemes, the vertex is a BH group. The black dot in the drawings represents a carbon atom. If a vertex contains an atom other than B and C, the heteroatom is shown explicitly. There are two cage-carbon-atom arrangements in carboranes, the carbon-atoms-adjacent (CAd) isomers where the cage carbon atoms occupy adjacent positions, and the carbon-atoms-apart (CAp) isomers where the cage carbon atoms are separated by at least one boron atom. For easy reference, all structurally characterized carboranes and metallacarboranes with more than 12 vertices are compiled in Tables 1–3 and included in the Supporting Information.

2. Carboranes with more than 12 vertices

2.1. Thirteen-vertex carboranes

Although *closo*-carboranes of the general formula $C_2B_nH_{n+2}$ have been known for $n = 3$–10 since the 1960s [3,4], knowledge of *closo*-carboranes and -boranes with more than 12 vertices has been limited merely to their possible cage geometries predicted by theoretical studies [27]. Recent calculations on boranes $B_nH_n^{2-}$ show that the overall stability of these clusters increases as n gets larger with the exception of $n = 12$ which is much more stable than the others [28]. Such an "icosahedral barrier" is often used to account for the failure in the syntheses of supercarboranes [22,29,30].

Recognition of the relatively lower reducing power of CAd carborane anions over the CAp counterparts offers a very valuable entry point to the synthesis of supercarboranes [31]. Accordingly, the first 13-vertex carborane 1,2-$C_6H_4(CH_2)_2$-5-Ph-1,2-$C_2B_{11}H_{10}$ was prepared by the Welch group in 6% yield from the reaction of [7,8-$C_6H_4(CH_2)_2$-7,8-$C_2B_{10}H_{10}$]Na_2 with $PhBCl_2$ [22] (Scheme 1). Single-crystal X-ray analyses show that the carborane cage of this molecule adopts a henicosahedral geometry, which is different from the predicted docosahedral geometry of $B_{13}H_{13}^{2-}$ [28]. DFT calculations reveal that the henicosahedral structure is preferred over the docosahedron by 7.4 KJ mol^{-1} for the 13-vertex carborane 1,2-$C_2B_{11}H_{13}$ (Scheme 2).

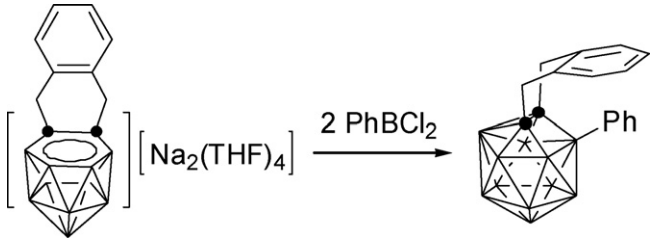

Scheme 1.

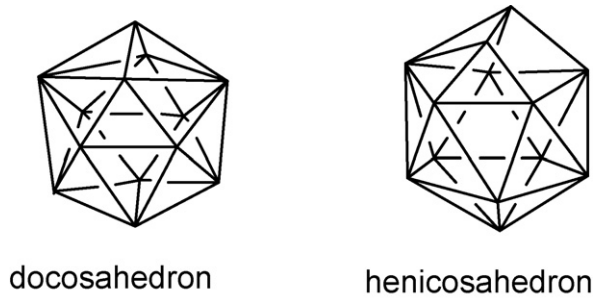

Scheme 2.

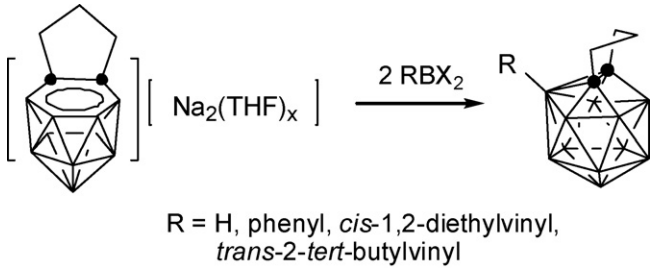

Scheme 3.

Subsequently, the Xie group synthesized a series of 13-vertex carboranes by treatment of the CAd carborane dianionic salts with borane dihalides in 7–32% yields using a trimethylene bridged carborane as the starting material [23,24] (Scheme 3). Non-donor solvents and less bulky borane reagents often offer higher synthetic yields. Fig. 1 shows the molecular structure of 1,2-$(CH_2)_3$-3-Ph-1,2-$C_2B_{11}H_{10}$ which is similar to that of 1,2-$C_6H_4(CH_2)_2$-5-Ph-1,2-$C_2B_{11}H_{10}$ [22]. The only difference in

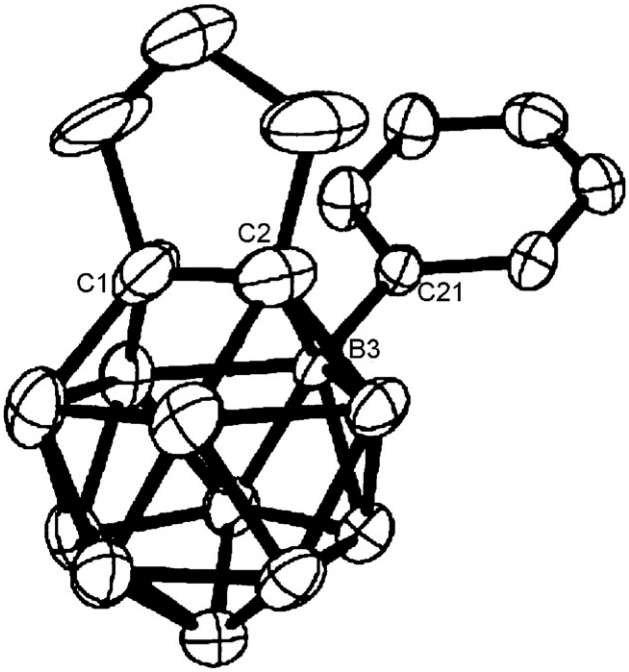

Fig. 1. Structure of 1,2-$(CH_2)_3$-3-Ph-1,2-$C_2B_{11}H_{10}$ reproduced by permission of The American Chemical Society from Ref. [24].

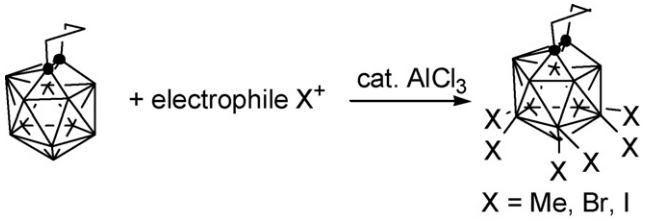

Scheme 4.

these two structures is the connectivity of the C(cage)–C(cage) moiety to its lower B_5 belt [24].

The Xie group also studied the reactivities of 13-vertex carboranes. Similar to 12-vertex ones, electrophilic substitutions are observed in the 13-vertex species [24]. Treatment of 1,2-$(CH_2)_3$-1,2-$C_2B_{11}H_{11}$ with excess MeI, Br_2, or I_2 in the presence of a catalytic amount of $AlCl_3$ gave the corresponding hexa-substituted 13-vertex carboranes 8,9,10,11,12,13-$(CH_3)_6$-1,2-$(CH_2)_3$-1,2-$C_2B_{11}H_5$, 8,9,10,11,12,13-Br_6-1,2-$(CH_2)_3$-1,2-$C_2B_{11}H_5$, or 8,9,10,11,12,13-I_6-1,2-$(CH_2)_3$-1,2-$C_2B_{11}H_5$, respectively [24], as shown in Scheme 4. The molecular structures of methyl- and bromo-substituted derivatives were confirmed by single-crystal X-ray analyses, which show that the substitution reactions take place at the B–H vertices that are the farthest away from the cage carbon atoms. This result is consistent with that found in *o*-carboranes. Fig. 2 shows the representative structure

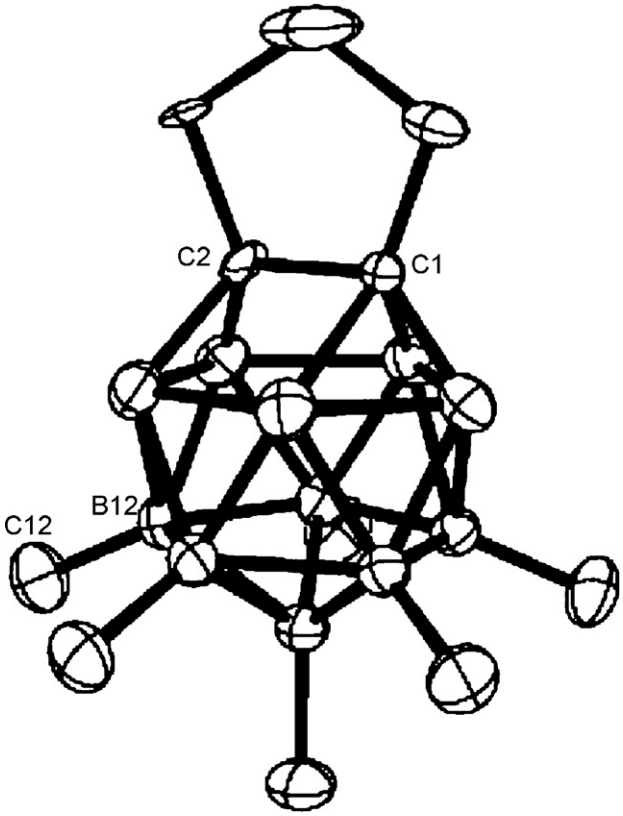

Fig. 2. Structure of 8,9,10,11,12,13-$(CH_3)_6$-1,2-$(CH_2)_3$-1,2-$C_2B_{11}H_5$ reproduced by permission of The American Chemical Society from Ref. [24].

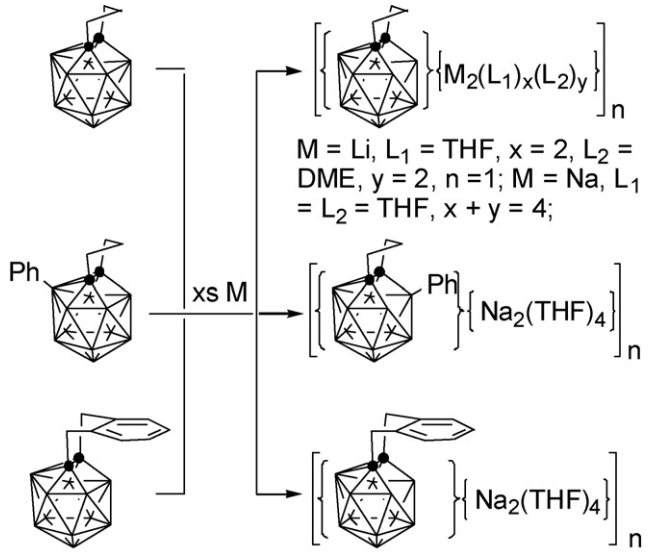

Scheme 5.

of the hexamethylated 13-vertex carborane. On the other hand, 13-vertex carboranes are chemically less stable than the 12-vertex ones. For example, they can be degraded by H_2O_2 and the hexa-halogenated species are found to be hygroscopic. These differences are ascribed to the joint effects of the nature of substituents and the more open trapezoidal faces presented in the 13-vertex carboranes [24].

Thirteen-vertex carboranes can be readily reduced by group 1 and 2 metals to yield the corresponding 13-vertex CAd *nido*-carborane salts [23,24] (Scheme 5). Such a reduction process is fast at room temperature even in the absence of naphthalene. As shown in Fig. 3, the *nido*-carborane dianion in the salts bears an open five-membered bent face with the out-of-plane (C(1)C(2)B(3)B(4)) displacement of B(8) atom ranging from 0.68 to 0.72 Å. Neither of the cations caps the open face, rather both coordinate to the peripheral terminal BH moieties affording the *exo-nido* species. Comparisons between the cage structures of the *closo* and *nido* species reveal that the reduction leads to the breaking of a B–B bond. In sharp contrast to the CAd 12-vertex *nido*-carboranes, the 13-vertex ones are resistant to further reduction by excess lithium metal. This result clearly indicates that the CAd 13-vertex *nido*-carboranes are stronger reducing agents (or weaker oxidants) than the CAd 12-vertex ones [24].

2.2. Fourteen-vertex carboranes

On the basis of the [12 + 1] protocol which has proven to be successful for the preparation of 13-vertex carboranes starting from CAd 12-vertex *nido*-carborane dianions, the Xie group subsequently developed a [12 + 2] methodology for the synthesis of 14-vertex carboranes [23]. Treatment of the 12-vertex CAd *arachno*-carborane tetraanionic salt [{1,2-$(CH_2)_3$-1,2-$C_2B_{10}H_{10}$}{$Li_4(THF)_5$}]$_2$ with 5 equiv. of $HBBr_2{\cdot}SMe_2$ led to the isolation of the first 14-vertex carborane 2,3-$(CH_2)_3$-2,3-$C_2B_{12}H_{12}$ and a 13-vertex one 1,2-$(CH_2)_3$-1,2-$C_2B_{11}H_{11}$ in 7% and 32% yields, respectively (Scheme 6). This 14-

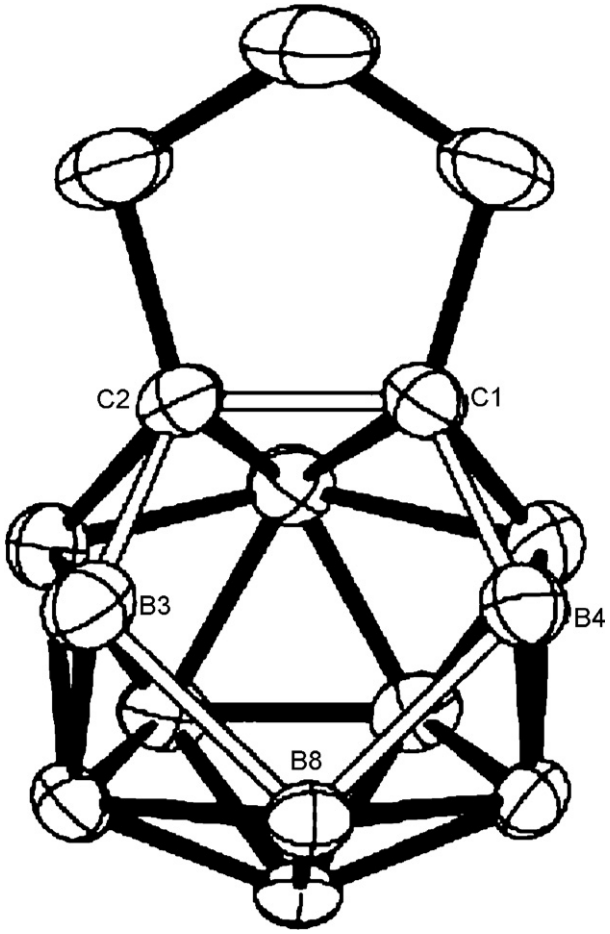

Fig. 3. Structure of $[1,2\text{-}(CH_2)_3\text{-}1,2\text{-}C_2B_{11}H_{11}]^{2-}$ reproduced by permission of Wiley–VCH from Ref. [23].

vertex carborane can also be synthesized from the reaction of the CAd 13-vertex *nido*-carborane dianionic salt $[\{nido\text{-}1,2\text{-}(CH_2)_3\text{-}1,2\text{-}C_2B_{11}H_{11}\}\{Na_2(THF)_4\}]_n$ with $HBBr_2{\cdot}SMe_2$ [23]. The oxidative cage closure is found to be a competitive reaction because of the strong reducing power of the *nido*-carborane anions. Fig. 4 shows the molecular structure of the 14-vertex carborane $2,3\text{-}(CH_2)_3\text{-}2,3\text{-}C_2B_{12}H_{12}$ [25]. It is a bicapped hexagonal antiprism molecule with all 24 faces being triangulated, which is consistent with that of $B_{14}H_{14}^{2-}$ predicted by theoretical calculations [28]. The two seven-coordinate boron atoms at the 1-and 14-positions engender longer B–C and B–B bonds with a distance of ∼1.90 Å.

These cage-expansion methods, which work well in the preparation of 13- and 14-vertex carboranes, have been unsuccessful when applied to the synthesis of 15-vertex ones [23–25]. Nonetheless, a CAd 14-vertex *nido*-carborane salt $[\{(CH_2)_3C_2B_{12}H_{12}\}\{Na_2(THF)_4\}]_n$ was obtained by treatment of the 14-vertex *closo*-carborane $2,3\text{-}(CH_2)_3\text{-}2,3\text{-}C_2B_{12}H_{12}$ with excess sodium metal in THF [25] (Scheme 7). As shown in Fig. 5, the CAd 14-vertex *nido*-carborane cage bears a bent five-membered open face which is bigger and flatter than that observed in the CAd 13-vertex *nido*-species. Reaction of this salt with $HBBr_2{\cdot}SMe_2$ did not produce any 15-vertex carborane, but rather afforded a structural isomer $2,8\text{-}(CH_2)_3\text{-}2,8\text{-}C_2B_{12}H_{12}$, confirmed by X-ray analyses [23], via the redox reaction (Scheme 7).

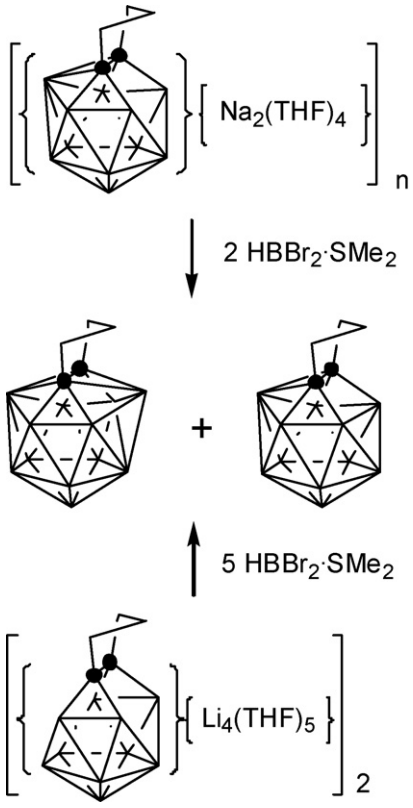

Scheme 6.

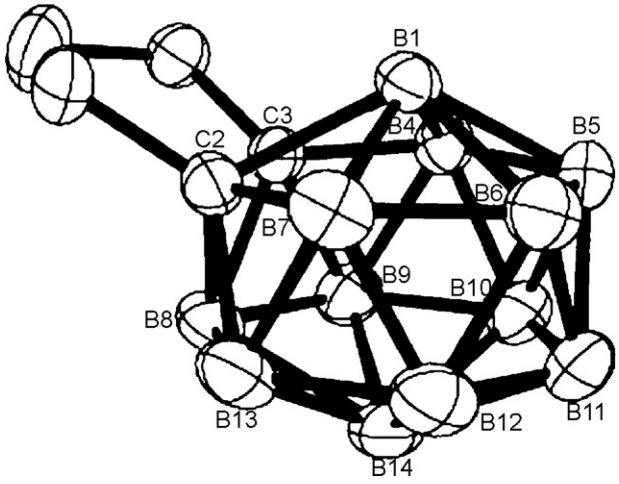

Fig. 4. Structure of $2,3\text{-}(CH_2)_3\text{-}2,3\text{-}C_2B_{12}H_{12}$ reproduced by permission of Wiley–VCH from Ref. [25].

3. Metallacarboranes with more than 12 vertices

Metallacarboranes with more than 12 vertices (so-called supermetallacarboranes) have been known much earlier than supercarboranes. Since the first report of a 13-vertex metallacarborane in 1971 [32], more than a hundred such complexes, several 14-vertex ones, and two 15-vertex examples have been

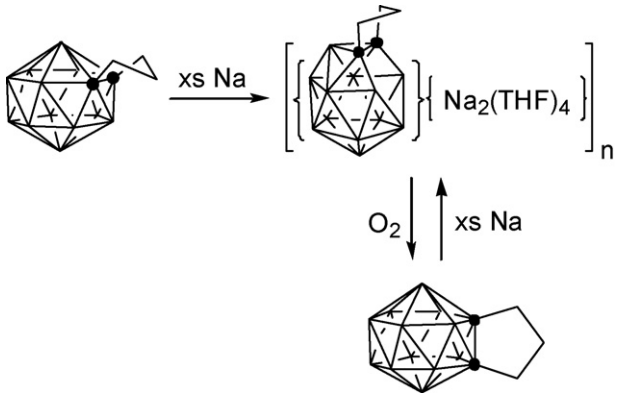

Scheme 7.

reported. The following discussion is arranged according to the cluster size and type of carborane ligand.

3.1. Thirteen-vertex metallacarboranes

The known 13-vertex metallacarboranes can be classified into five types: MC_2B_{10}, MC_4B_8, $M_2C_3B_8$, $M_2C_2B_9$, and $M_3C_3B_7$ with the MC_2B_{10} system being in the majority.

3.1.1. MC_2B_{10} system

Metallacarboranes of the MC_2B_{10} type encompass main group metals, most transition metals, lanthanides, and actinides,

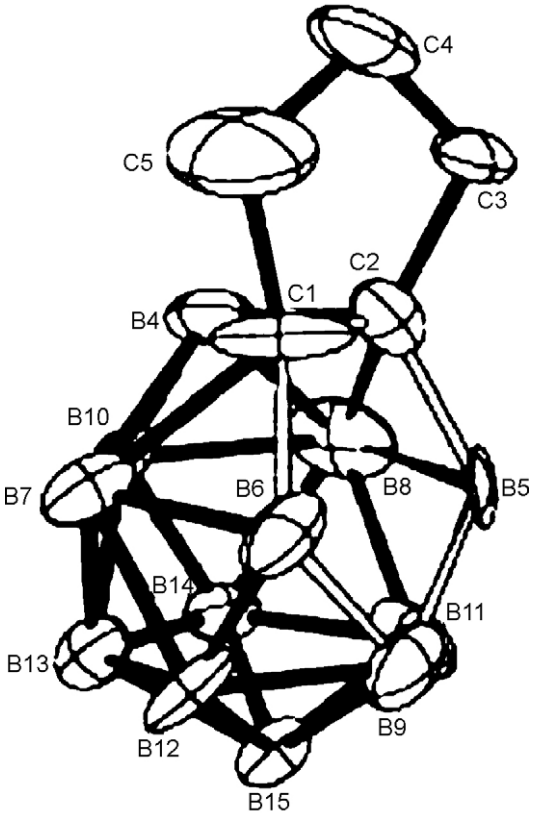

Fig. 5. Structure of $[(CH_2)_3C_2B_{12}H_{12}]^{2-}$ reproduced by permission of Wiley–VCH from Ref. [25].

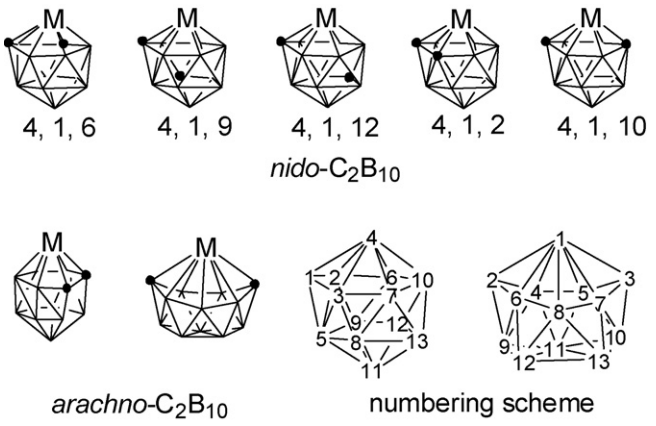

Scheme 8.

and display versatile cage geometries with various bonding modes. Scheme 8 illustrates common cluster geometries and the numbering systems.

3.1.1.1. MC_2B_{10} system bearing nido-C_2B_{10} ligand. Complex 4-Cp-4,1,6-$CoC_2B_{10}H_{12}$, synthesized in 1971 by the Hawthorne group [32] and structurally characterized by an X-ray diffraction study in 1972 [33], is the first example of heteroborane cluster with 13 vertices. Reduction of *o*-$C_2B_{10}H_{12}$ with sodium metal followed by capitation reaction with $CoCl_2$/CpNa resulted in the formation of a Co(III) complex 4-Cp-4,1,6-$CoC_2B_{10}H_{12}$, which was successively converted into another two structural isomers upon heating [32] (Scheme 9). The structures of these two isomers have not been confirmed by X-ray analyses owing to positional disorder problems. A parallel study on the Cp* analogs was recently reported [34], which identified the structural isomers as 4-Cp*-4,1,6-$CoC_2B_{10}H_{12}$, 4-Cp*-4,1,9-$CoC_2B_{10}H_{12}$, and 4-Cp*-4,1,12-$CoC_2B_{10}H_{12}$. Fig. 6 shows the molecular structure of 4-Cp-4,1,6-$CoC_2B_{10}H_{12}$, in which the cobalt atom is bonded to the Cp and carboranyl ligand in η^5- and η^6-fashion, respectively, with the Co–Cent distances of 1.65 and 1.34 Å. The six-membered C_2B_4 face is nearly coplanar with the C(1) vertex being slightly out of the plane. This engenders a relatively short Co–C(1) distance of 2.032(4) Å, while the other Co–cage atom distances range from 2.093(3) to 2.199(6) Å [33].

Using CAp [*nido*-7,9-$C_2B_{10}H_{12}]^{2-}$ as a ligand, the Hawthorne group prepared a series of 13-vertex metallacarboranes of the 4,1,6-type including both half- and full-sandwich complexes (η^5-Cp)Fe(η^6-$C_2B_{10}H_{12}$), $[NMe_4][(\eta^5\text{-Cp})Fe(\eta^6\text{-}C_2B_{10}H_{12})]$, $[NEt_4]_2[(CO)_3Mo(\eta^6\text{-}C_2B_{10}H_{12})]$, $[NEt_4]_2[(CO)_3W(\eta^6\text{-}C_2B_{10}H_{12})]$, $[NEt_4]_2[Fe(\eta^6\text{-}C_2B_{10}H_{12})_2]$,

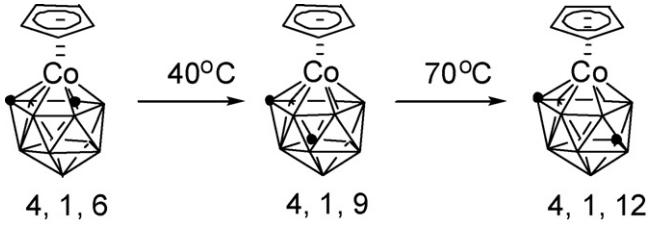

Scheme 9.

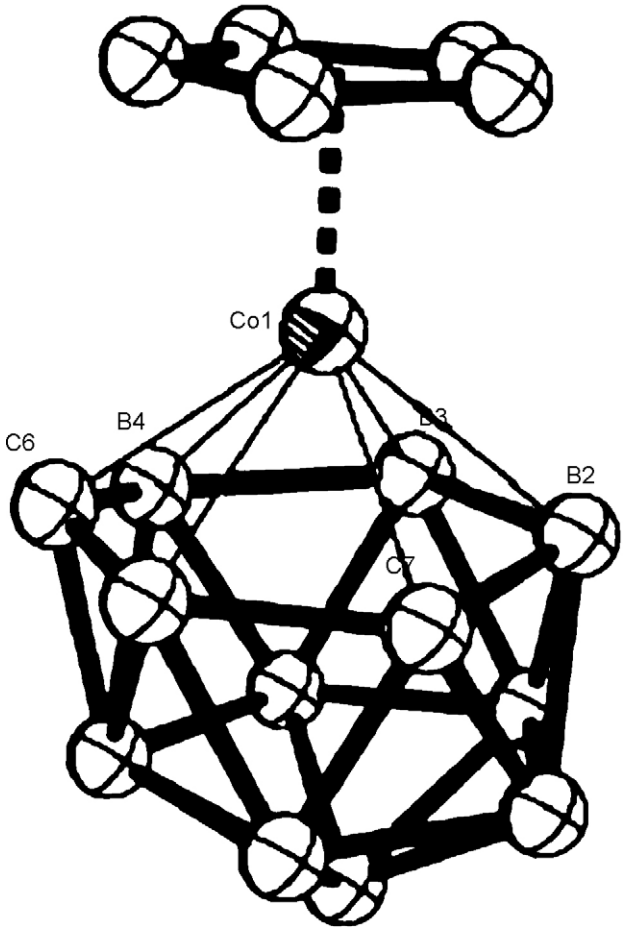

Fig. 6. Structure of 4-Cp-4,1,6-$CoC_2B_{10}H_{12}$ reproduced by permission of The Royal Society of Chemistry from Ref. [33].

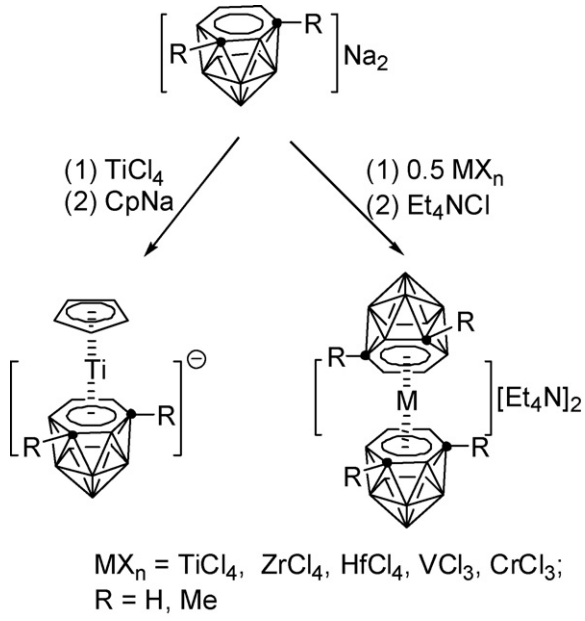

Scheme 10.

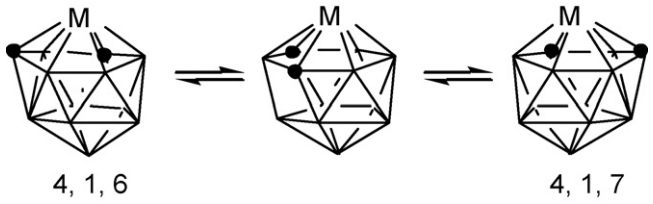

Scheme 11.

$[NEt_4][Co(\eta^6\text{-}C_2B_{10}H_{12})_2]$, $[NEt_4]_2[Ni(\eta^6\text{-}C_2B_{10}H_{12})_2]$, and $Ni(\eta^6\text{-}C_2B_{10}H_{12})_2$ [35]. The synthesis and characterization of early transition metal analogs $[NEt_4]_2[M(\eta^6\text{-}R_2C_2B_{10}H_{10})_2]$ (M = Ti, V, Cr, Mn, Zr, Hf; R = H or Me), $[NEt_4][(L)Ti(\eta^6\text{-}R_2C_2B_{10}H_{10})]$ (L = C_5H_5, C_8H_8; R = H or Me), and $(C_8H_8)Ti(\eta^6\text{-}C_2B_{10}H_{12})$, all as the 4,1,6-isomers, are also described [36–38] (Scheme 10). It is noted that a significant amount of *o*-carborane is generated during the reactions, which results from the redox reactions between the CAp *nido*-carborane dianion and high-valent early transition metal halides [36,38]. Among these complexes, the structure of the sandwich Ti(II) complex $[NEt_4]_2[Ti(\eta^6\text{-}Me_2C_2B_{10}H_{10})_2]$ has been confirmed by single-crystal X-ray analyses [37]. Similar to the 13-vertex cobaltacarborane, a rapid interconversion between the 4,1,6- and 4,1,7-isomers at room temperature in solution is found in the early transition metal complexes as their ^1H NMR spectra show only one singlet for two C(cage)–H or C(cage)–CH_3 units [36] (Scheme 11). They also undergo a facile 4,1,6- to 4,1,9- to 4,1,12- polyhedral rearrangement in solution at elevated temperatures [38].

These seminal studies laid the foundation for further exploration on supermetallacarboranes. The introduction of ancillary ligands to metal centers before capitation results in the clean formation of 13-vertex metallacarboranes as the ancillary ligands can not only make the metal ions more resistant to redox reactions but also stabilize the resultant 13-vertex metallacarboranes. Thus, a large number of late transition metal complexes of the type MC_2B_{10} (M = Mo, W, Mn, Re, Fe, Ru, Co, Rh, Ir, Ni, Pd) were obtained. The neutral complexes such as 4-arene-1,6-R_2-4,1,6-$RuC_2B_{10}H_{10}$, (arene = C_6H_6, *p*-cymene; R = H, Ph) [39], 4-H-4,4-$(PPh_3)_2$-4,1,6-$RhC_2B_{10}H_{12}$ [40], 4-H-4,4-$(PPh_3)_2$-2-(MeO)-4,1,6-$IrC_2B_{10}H_{11}$ [41], and 4-dppe-4,1,6-$PdC_2B_{10}H_{12}$ [41] were generally synthesized by salt metathesis. In the preparation of the rhoda- and iridacarborane, an oxidative addition reaction was involved when treating $ClM(PPh_3)_3$ (M = Rh, Ir) with $[NMe_4][C_2B_{10}H_{13}]$ as shown in Scheme 12. Fig. 7 shows the molecular structure of the rhodium complex [40]. As the cage fluxionality and isomerization are often observed in 13-vertex metallacarboranes, it is interesting to note that both ruthenacarborane and rhodacarborane are thermally stable. These results illustrate the effects of metal centers and ancillary ligands on the stability of 13-vertex metallacarboranes.

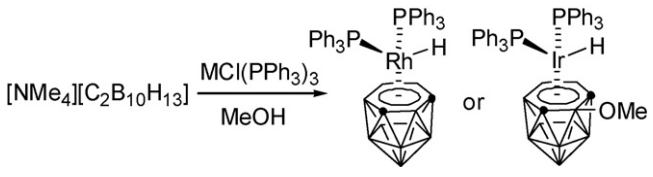

Scheme 12.

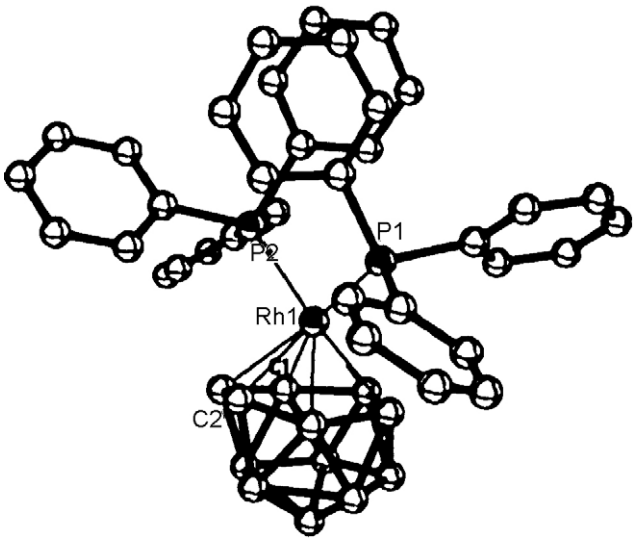

Fig. 7. Structure of 4-H-4,4-$(PPh_3)_2$-4,1,6-$RhC_2B_{10}H_{12}$ reproduced by permission of The American Chemical Society from Ref. [40].

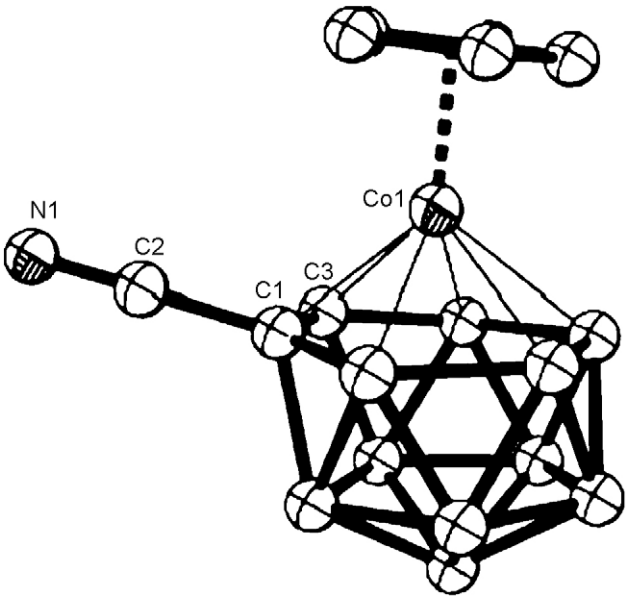

Fig. 8. Structure of 4-Cp-1-CN-4,1,2-$CoC_2B_{10}H_{11}$ reproduced by permission of Elsevier from Ref. [43].

The neutral 13-vertex metallacarboranes of the late transition metals of the 4,1,2- and 4,1,10-type are also known. Reaction of 1-Me-1,2-$C_2B_{10}H_{11}$ with 2 equiv. of $Co(PEt_3)_4$ in toluene afforded a 13-vertex species $(\eta^6\text{-}MeC_2B_{10}H_{11})Co_2(PEt_3)_3$ [42]. This cobaltacarborane is suggested to be the 4,1,2-type, although one of the cage carbon atoms is not unambiguously located. A well characterized CAd 13-vertex cobaltacarborane 4-Cp-1-CN-4,1,2-$CoC_2B_{10}H_{11}$ was prepared from the CAd *arachno*-C_2B_{10} anion [43] (Scheme 13). Fig. 8 shows its molecular structure. The adjacent positions of the two cage carbon atoms lead to a relatively short C(cage)–C(cage) distance of 1.45 Å. This structural feature is also found in other C,C′-linked 13-vertex metallacarboranes of the 4,1,2-type. Reduction of the tethered carborane 1,2-$(CH_2)_3$-1,2-$C_2B_{10}H_{10}$ with excess sodium metal, followed by treatment with metal halides afforded 13-vertex metallacarboranes 4-L-1,2-$(CH_2)_3$-4,1,2-$MC_2B_{10}H_{10}$ (L = Cp, M = Co; L = *p*-cymene, M = Ru; L = $(PMe_2Ph)_2$, M = Pt; L = dppe, M = Ni) [44] (Scheme 14). They are well characterized spectroscopically and crystallographically.

Thirteen-vertex metallacarboranes of the 4,1,10-MC_2B_{10} type were recently reported by the Welch group [45]. Reduction of 1,12-R_2-1,12-$C_2B_{10}H_{10}$ (R = H or Me) with sodium metal in liquid ammonia followed by metallation in THF gave 13-vertex complexes 4-L-1,10-R_2-4,1,10-$MC_2B_{10}H_{10}$ (L = Cp, M = Co, R = H; L = *p*-cymene, M = Ru, R = H; L = C_6H_6, M = Ru, R = Me; L = C_6Me_6, M = Ru, R = Me; L = dppe, M = Ni, R = H) (Scheme 15). Fig. 9 shows the representative structure of the Co species [45]. These complexes can be readily converted into the 4,1,12-isomers upon heating, which serves a new entry point to the 4,1,12-species. Fig. 10 shows the molecular structure of a ruthenacarborane of this type [45].

The Stone group prepared a series of anionic 13-vertex metallacarboranes. Treatment of CAp $Na_2[Me_2C_2B_{10}H_{10}]$ with $M(\equiv CR)Cl(CO)_2(py)_2$ (M = Mo or W; R = 4-Me-C_6H_4 or 2,6-Me_2-C_6H_3; py = pyridine or 4-Me-pyridine) followed by addition of $[NEt_4]Cl$ generated 13-vertex metallacarborane salts $[NEt_4][4\text{-}(\equiv CR)\text{-}4,4\text{-}(CO)_2\text{-}1,6\text{-}Me_2\text{-}4,1,6\text{-}MC_2B_{10}H_{10}]$ [46,47] (Scheme 16). Fig. 11 shows the molecular structure of the complex anion in $[NEt_4][4\text{-}(\equiv CC_6H_3\text{-}2,6\text{-}Me_2)\text{-}4,4\text{-}(CO)_2\text{-}1,6\text{-}Me_2\text{-}4,1,6\text{-}WC_2B_{10}H_{10}]$, in which the carborane anion is η^6-bound to the tungsten atom forming a 13-vertex cage [46]. The metal-carbyne moieties in these 13-vertex metallacarboranes have proven to be useful for the construction of multi-nuclear metal complexes. As shown in Scheme 17, the anionic tungsten species can readily react with various kinds of late transition metal compounds to give binuclear complexes holding versatile W–C–M triangles (M = Mo, W, Fe, Co, Rh, Pt, Au) [47–50]. The BH moiety on the C_2B_4 open face may also be involved in bonding with the incoming metal fragment, which is demonstrated by both NMR

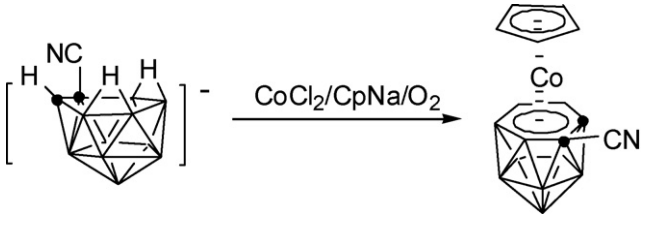

Scheme 13.

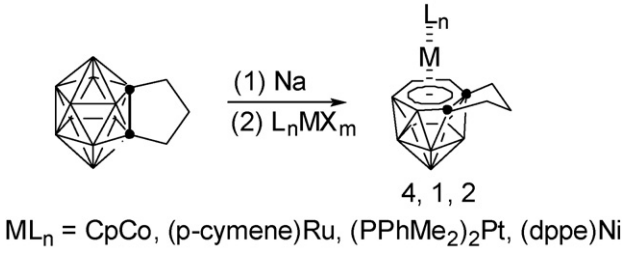

Scheme 14.

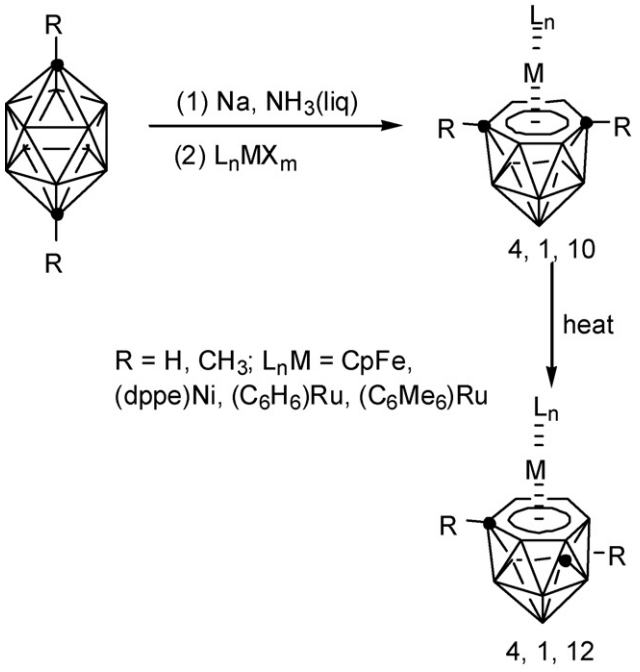

Scheme 15.

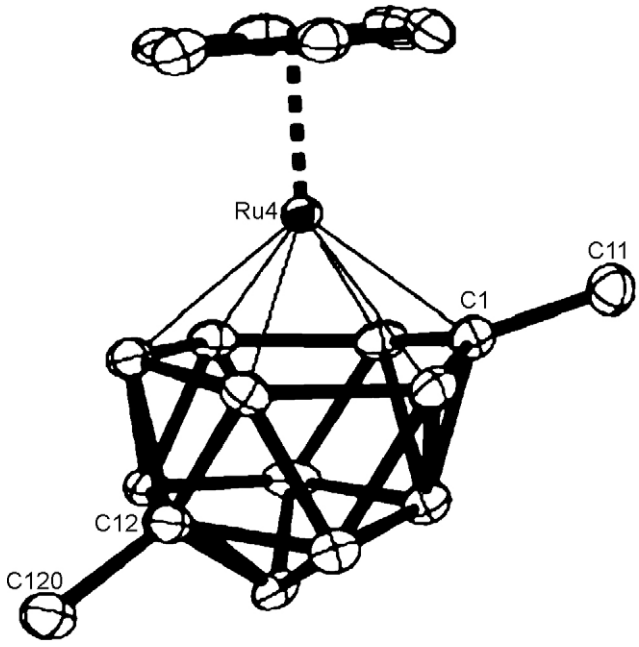

Fig. 10. Structure of 4-C_6H_6-1,12-Me_2-4,1,12-$RuC_2B_{10}H_{10}$ reproduced by permission of The Royal Society of Chemistry from Ref. [45].

studies and single-crystal X-ray analyses. In some cases, the BH moiety can even be activated as observed in the platinum-containing complex, (μ-σ:η^6-$Me_2C_2B_{10}H_9$)WPt(μ-CC_6H_4Me-4)$(CO)_4(CO)_2(PMe_2Ph)_2$ [49]. Generally, the incorporation of new metal fragments has no significant effect on the geometry of the original metallacarboranes.

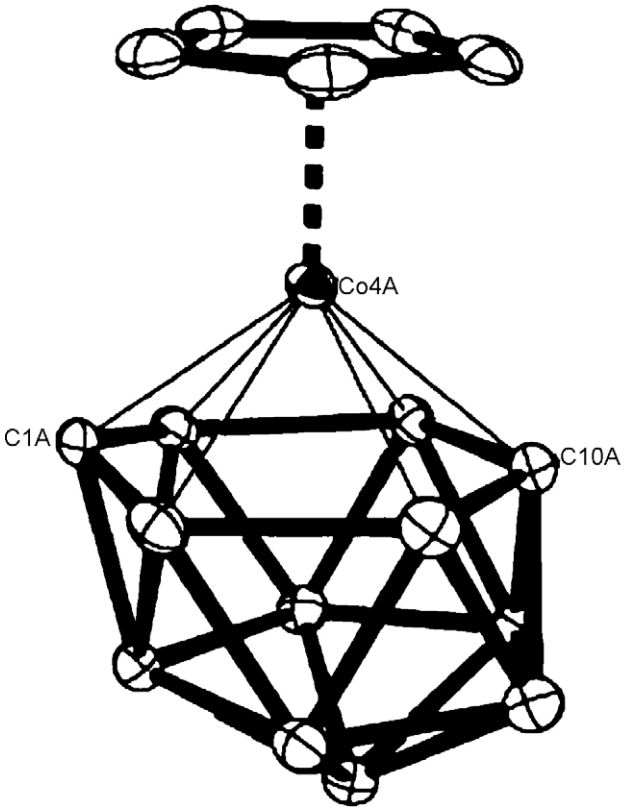

Fig. 9. Structure of 4-Cp-4,1,10-$CoC_2B_{10}H_{12}$ reproduced by permission of The Royal Society of Chemistry from Ref. [45].

The 13-vertex alkylidynyl tungstacarboranes [NEt_4][4-(≡CR)-4,4-$(CO)_2$-1,6-R'_2-4,l,6-$WC_2B_{10}H_{10}$] (R = C_6H_3-2,6-Me_2, Me; R′ = Me, H) undergo a facile proton-induced degradation in the presence of donor molecules L (L = CO, PhC≡CPh, PPh_3) to give neutral 12- or 13-vertex tungstacarboranes depending on the properties of L [51,52]. As shown in Scheme 18, the resultant 13-vertex metallacarboranes have the general formula 4-L-4,4-$(CO)_2$-1,6-R'_2-7-CH_2R-4,1,6-$WC_2B_{10}H_9$, which may result from the migration and insertion into the B(7)–H bond of an initially formed alkylidene {CHR} group. These complexes are thermally unstable and

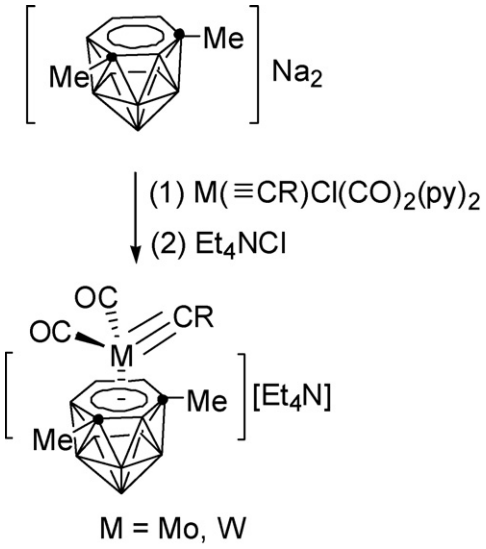

Scheme 16.

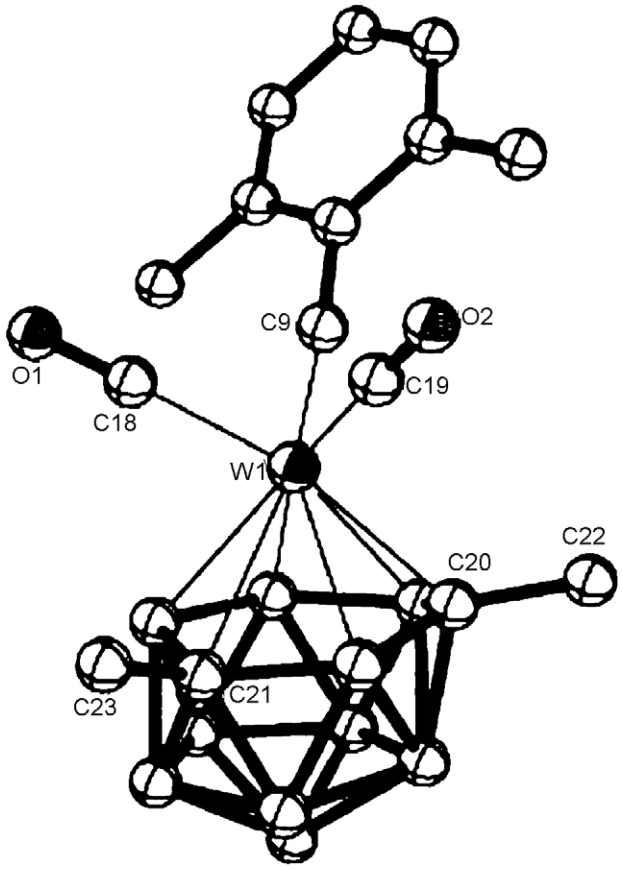

Fig. 11. Structure of $[4\text{-}(\equiv CC_6H_3\text{-}2',6'\text{-}Me_2)\text{-}4,4\text{-}(CO)_2\text{-}1,6\text{-}Me_2\text{-}4,1,6\text{-}WC_2B_{10}H_{10}]^-$ reproduced by permission of Elsevier from Ref. [46].

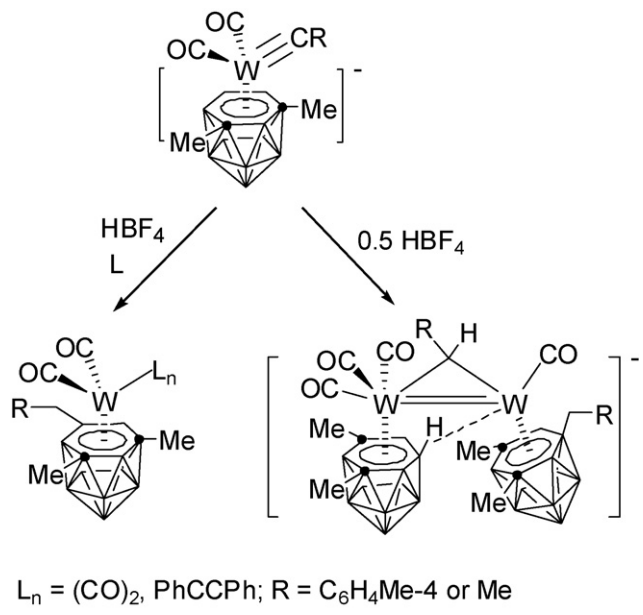

Scheme 18.

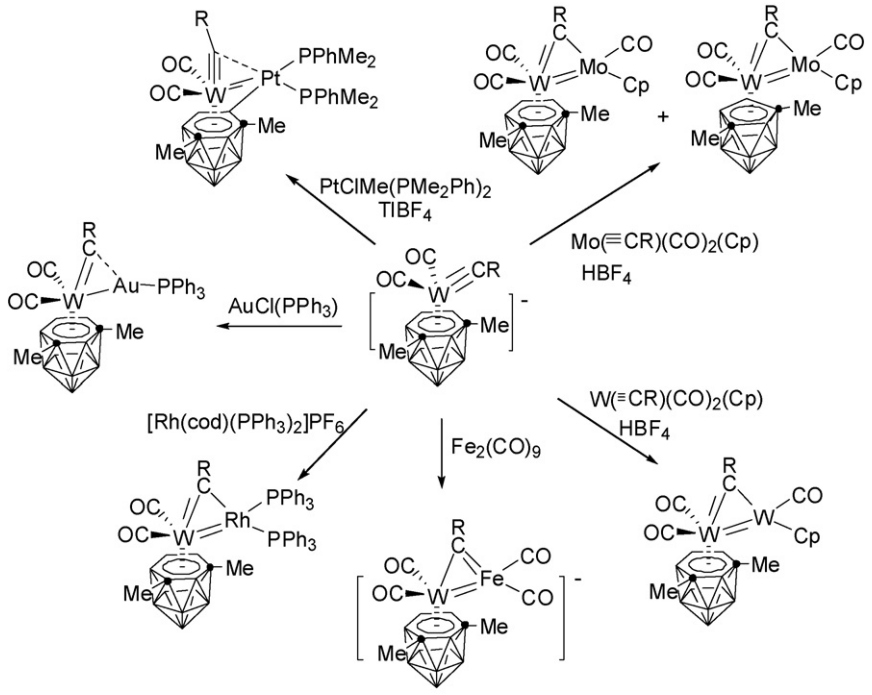

Scheme 17.

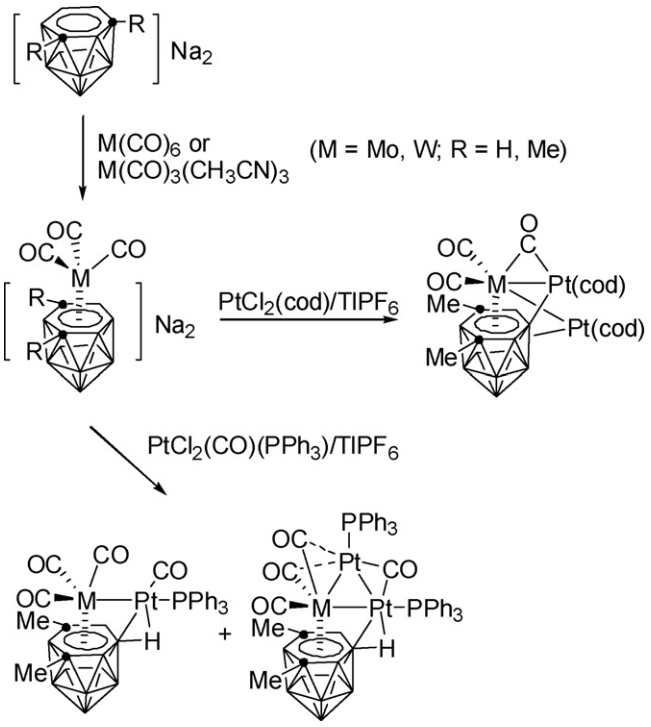

Scheme 19.

slowly decompose to give 12-vertex tungstacarboranes with a 2,1,7-WC_2B_9 cage framework by loss of both a BH fragment and CHR moiety [51]. Protonation with 0.5 equiv. of HBF_4 in the absence of donor molecules afforded a ditungsten complex whose structure has been confirmed by X-ray analyses [52].

In addition to the alkylidynyl 13-vertex molyda- and tungstacarboranes, the Stone group synthesized the tricarbonyl analogs in good yield using $M(CO)_3(CH_3CN)_3$ (M = Mo, W) as starting materials [53]. The syntheses of the di- and tri-metallic complexes were achieved [53,54] (Scheme 19). The allyl group can also been incorporated into the 13-vertex metallacarboranes as an ancillary ligand. The ammonium salts of [4-(η^3-C_3H_5)-4,4-$(CO)_2$-1,6-Me_2-4,1,6-$MC_2B_{10}H_{10}]^-$ (M = Mo, W) [55,56] and [4-(η^3-C_3H_5)-1,6-Me_2-4,1,6-$MC_2B_{10}H_{10}]^-$ (M = Ni, Pd) [57] were prepared by treatment of $Na_2[Me_2C_2B_{10}H_{10}]$ with the corresponding allyl metal halides (Scheme 20). Fig. 12

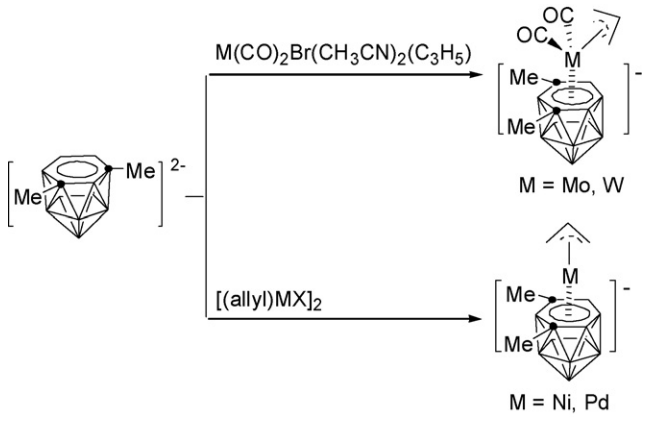

Scheme 20.

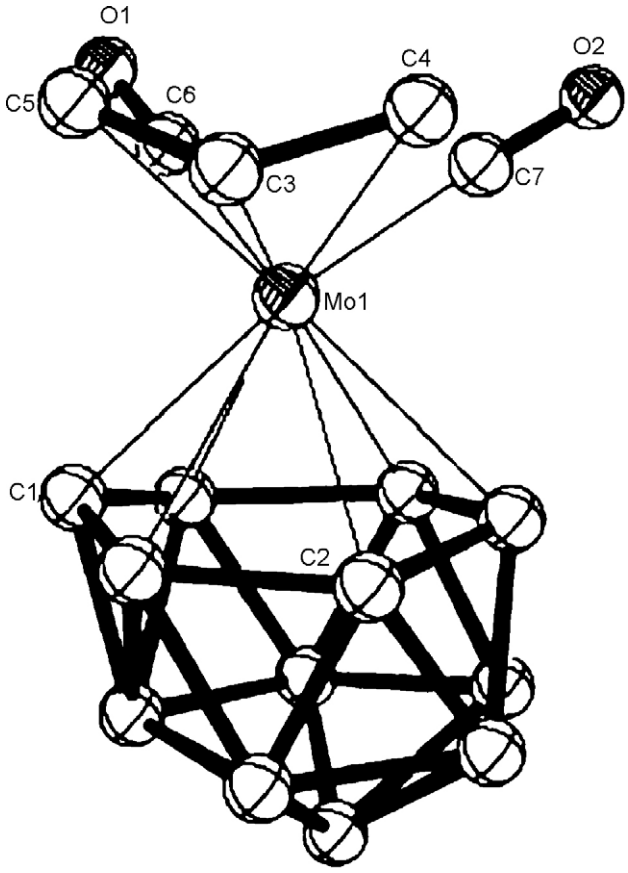

Fig. 12. Structure of [4-(η^3-C_3H_5)-4,4-$(CO)_2$-1,6-Me_2-4,1,6-$MoC_2B_{10}H_{10}]^-$ reproduced by permission of Elsevier from Ref. [56].

shows the molecular structure of the allyl molybdenum complex [56]. Protonation of the anionic allyl molydacarborane with HBr at ambient atmosphere of CO yielded a neutral 13-vertex molydacarborane 4-Br-4,4,4-$(CO)_3$-1,6-Me_2-4,1,6-$MoC_2B_{10}H_{10}$ whose structure has been confirmed by an X-ray diffraction study [55]. The anionic allyl palladacarborane is unstable, whereas the nickel species has good thermal stability. The latter is used to prepare dimetallic complexes by treating with mono-cationic metal fragments [58], as shown in Scheme 21. There is no metal–metal bond in these hetero dinuclear species and the exopolyhedral Cu, Rh, and Ru fragments are attached to the nickelacarborane cluster via B–H–M interactions. Although the NMR experiments reveal the presence of several isomers in solution, recrystallization of these dinuclear species lead to the formation of a unique isomer as indicated by single-crystal X-ray analyses.

The Stone group recently reported the 13-vertex complex anions [4,4,4-$(CO)_3$-4,1,6-$MC_2B_{10}H_{12}]^-$ (M = Mn, Re) [59] and [4-(cod)-4,1,6-$RhC_2B_{10}H_{12}]^-$ [60] prepared by salt metathesis shown in Schemes 22 and 23. The rhena- and rhodacarborane anions can react with cations to yield neutral bimetallic species with or without a metal–metal bond depending on the nature of metals [59,60]. Reactions on the carborane cage and ancillary ligands were also studied. The BH vertex at the 7-position of the 13-vertex rhena- or rhodacarborane anion

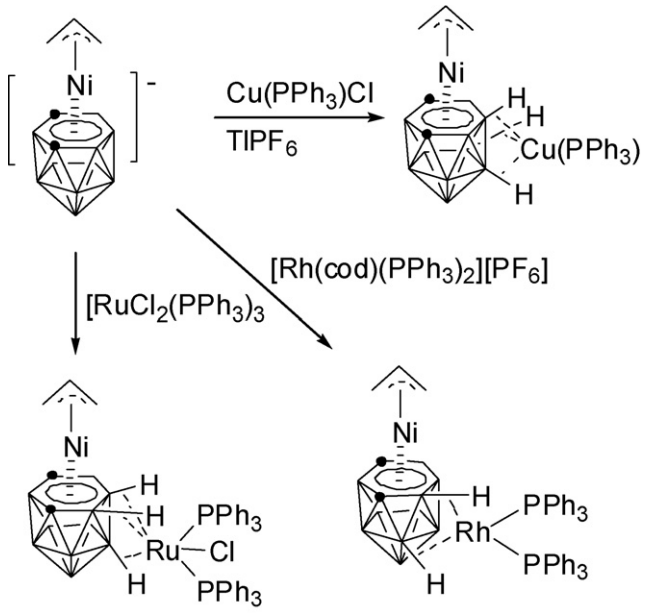

Scheme 21.

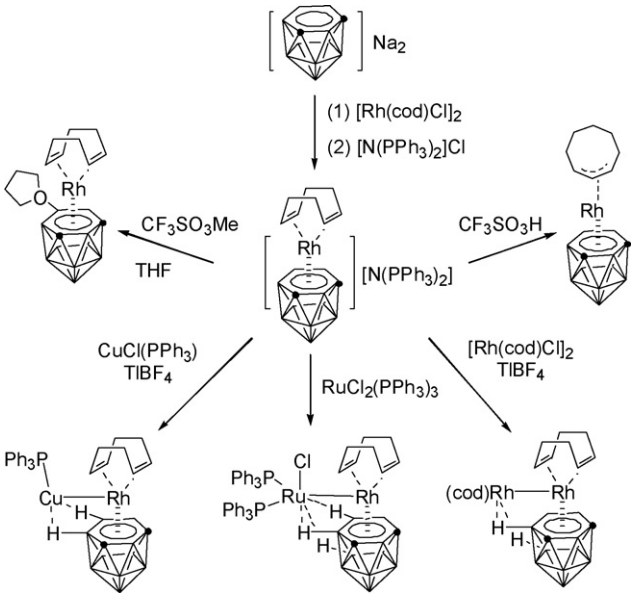

Scheme 23.

is very reactive and can be attacked by electrophiles to give substitution products (Schemes 22 and 23).

Thirteen-vertex metallacarboranes of coinage metals and p-block elements are quite rare. $[N(CH_2Ph)Et_3][4\text{-}PPh_3\text{-}1,6\text{-}Me_2\text{-}4,1,6\text{-}AuC_2B_{10}H_{10}]$ [61], $4\text{-}PPh_3\text{-}4,7,10\text{-}\{Cu(PPh_3)\}\text{-}7,10\text{-}(\mu\text{-}H)_2\text{-}4,1,6\text{-}CuC_2B_{10}H_{10}$ [59], $1,6\text{-}R_2\text{-}4,1,6\text{-}SnC_2B_{10}H_{10}$ (R = Me, H) [62], and $1,2\text{-}\{o\text{-}(CH_2)_2C_6H_4\}\text{-}4,1,2\text{-}SnC_2B_{10}H_{10}$ [63] are the only known examples. The gold species was obtained by the reaction of CAp *nido*-carborane dianion with $ClAu(PPh_3)$. As shown in Fig. 13, the $Au(PPh_3)$ fragment is only bonded to the *nido*-carborane cage in η^3-fashion with an average Au–B distance of 2.388(7) Å [61]. The slipped structure can be ascribed to the electron-richness of the d^{10} metal center. The 13-vertex cupracarborane was unexpectedly isolated as a by-product from the reaction of 13-vertex rhenacarborane anion with $[Cu(PPh_3)]^+$ [59]. As this species cannot be directly synthesized from the reaction of CAp *nido*-$[C_2B_{10}H_{12}]^{2-}$ with $[Cu(PPh_3)]^+$, which only gave *o*-carborane, a 14-vertex $\{ReCuC_2B_{10}\}$ cluster is then speculated as an intermediate which may extrude the rhenium to produce the 13-vertex copper complex. The structure of this cupracarborane is different from that of the gold one as the η^6-bonding interaction is observed between the *nido*-carborane cage and

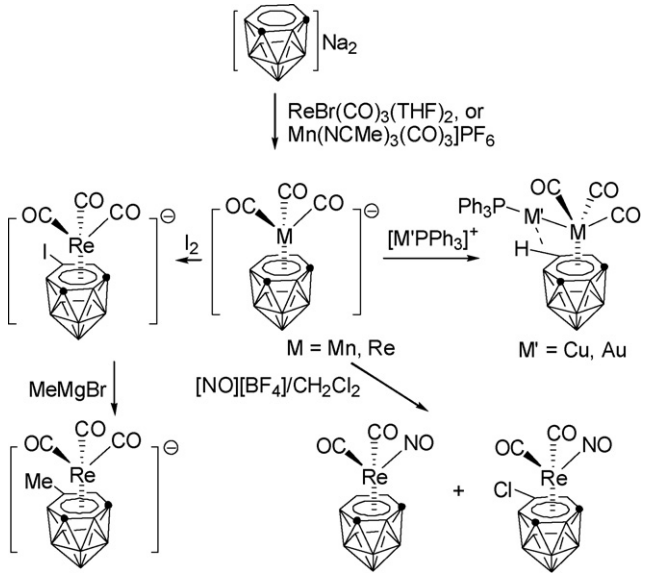

Scheme 22.

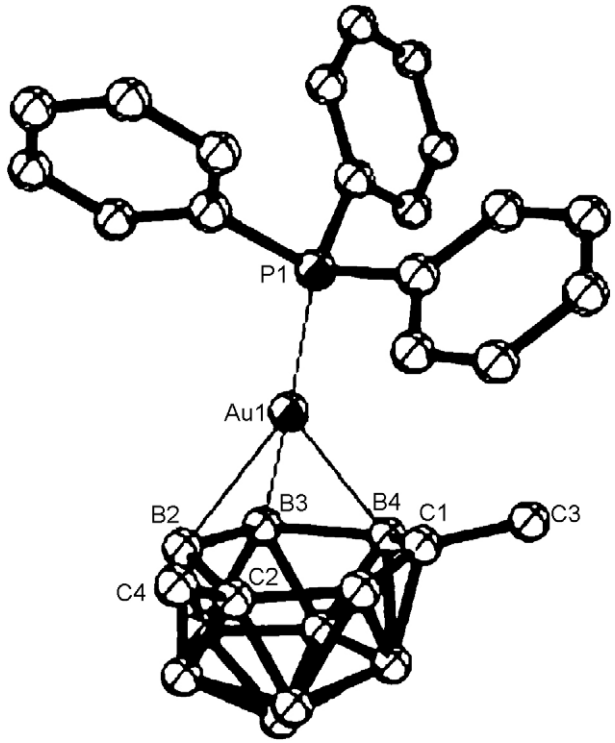

Fig. 13. Structure of $[(PPh_3)Au(\eta^3\text{-}Me_2C_2B_{10}H_{10})]^-$ reproduced by permission of The American Chemical Society from Ref. [61].

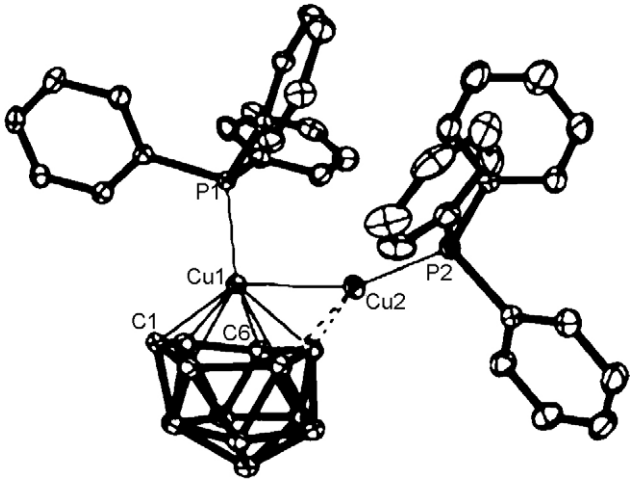

Fig. 14. Structure of $[(PPh_3)Cu(\eta^6\text{-}C_2B_{10}H_{12})]Cu(PPh_3)$ reproduced by permission of The American Chemical Society from Ref. [59].

one of the $Cu(PPh_3)$ fragments. The other $Cu(PPh_3)$ unit is supported by a Cu–Cu bond and the B–H–Cu interaction [59] (Fig. 14). Reaction of $Na_2[7,9\text{-}R_2\text{-}7,9\text{-}C_2B_{10}H_{10}]$ (R = H, Me) with $SnCl_2$ in THF afforded $1,6\text{-}R_2\text{-}4,1,6\text{-}SnC_2B_{10}H_{10}$. X-ray analyses reveal that the tin atom is η^6-bound to the carboranyl ligand and is free of solvation [62]. On the other hand, treatment of $Na_2[7,8\text{-}\{(CH_2)_2C_6H_4\}\text{-}7,8\text{-}C_2B_{10}H_{10}]$ with $SnCl_2$ gave $4\text{-L-}1,2\text{-}\{o\text{-}(CH_2)_2C_6H_4\}\text{-}4,1,2\text{-}SnC_2B_{10}H_{10}$ (L = THF, DME, MeCN), in which the Sn atom has slipped away from the top of the C_2B_4 bonding face [63] (Scheme 24).

Group 1 metal salts $M_2[7,9\text{-}C_2B_{10}H_{12}]$ are very useful synthons for the production of 13-vertex metallacarboranes of alkaline-earth metals and lanthanides. Treatment of MI_2 with 1 equiv. of CAp $Na_2[nido\text{-}C_2B_{10}H_{12}]$ in THF resulted in the isolation of metallacarboranes $4\text{-}(THF)_x\text{-}4,1,6\text{-}MC_2B_{10}H_{12}$ (M = Ca [64], Sr [65], Sm, Eu, Yb [66]) (Scheme 25). Recrystallization of these complexes from $MeCN/Et_2O$ gave MeCN coordinated species. The molecular structures of $[4,4,4\text{-}(MeCN)_3\text{-}4,1,6\text{-}MC_2B_{10}H_{12}]_n$ (M = Sr, Eu) and $4,4,4,4\text{-}(MeCN)_4\text{-}4,1,6\text{-}CaC_2B_{10}H_{12}$ have been confirmed by single-crystal X-ray analyses. Fig. 15 shows the structure of the Eu species [66]. The average Eu–N and Eu–cage atom distances are 2.677(9) and 2.983(11) Å, respectively. The full-sandwich lanthanacarborane ion $[(\eta^6\text{-}C_2B_{10}H_{12})_2Eu(THF)_2]^{2-}$ of the 1,6-type was obtained by either the reaction of

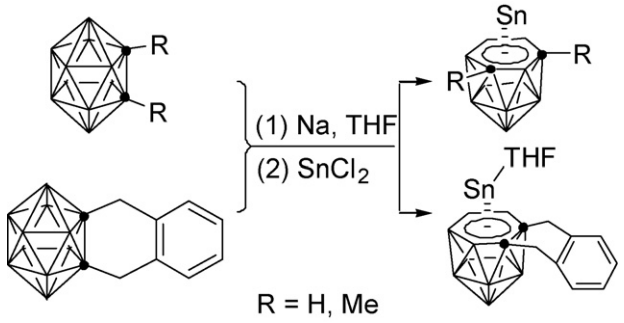

Scheme 24.

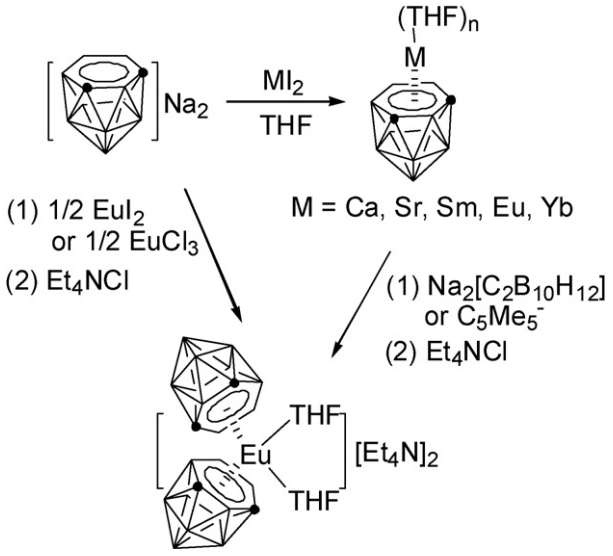

Scheme 25.

half-sandwich species with an equimolar amount of CAp $Na_2[nido\text{-}C_2B_{10}H_{12}]$, or the reaction of $EuCl_3$ with 2 equiv. of CAp $nido\text{-}C_2B_{10}H_{12}^{2-}$ (Scheme 25), whose structure has been confirmed by single-crystal X-ray analyses as an ammonium salt [66].

Substituents on the cage carbon atoms play an important role in the bonding interactions between the lanthanide and carboranyl ligand. Reaction of CAp $[nido\text{-}7,9\text{-}(PhCH_2)_2\text{-}7,9\text{-}C_2B_{10}H_{10}]^{2-}$ with LnI_2 (Ln = Sm, Yb) did not give the expected 13-vertex lanthanacarboranes, rather afforded $exo\text{-}nido\text{-}[7,9\text{-}(PhCH_2)_2\text{-}7,9\text{-}C_2B_{10}H_{10}][Ln(DME)_3]$ [67]. However, treatment of $SmCl_3$ with 2 equiv. of CAp $[nido\text{-}7,9\text{-}(PhCH_2)_2\text{-}7,9\text{-}C_2B_{10}H_{10}]Na_2(THF)_4$ in THF yielded an unprecedented cluster $closo\text{-}exo\text{-}[(PhCH_2)_2C_2B_{10}H_{10}]_4Sm_2Na_3$ [67] (Scheme 26). It is a mixed-valent samaracarborane containing both Sm(III) and

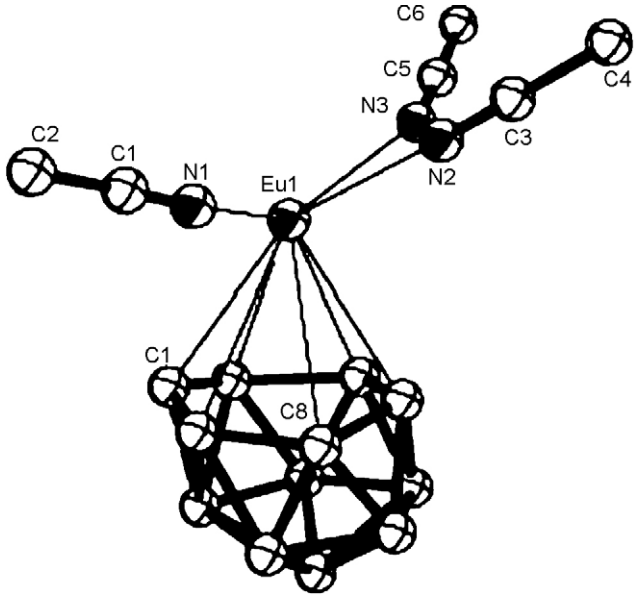

Fig. 15. Structure of $(\eta^6\text{-}C_2B_{10}H_{12})Eu(MeCN)_3$ reproduced by permission of The American Chemical Society from Ref. [66].

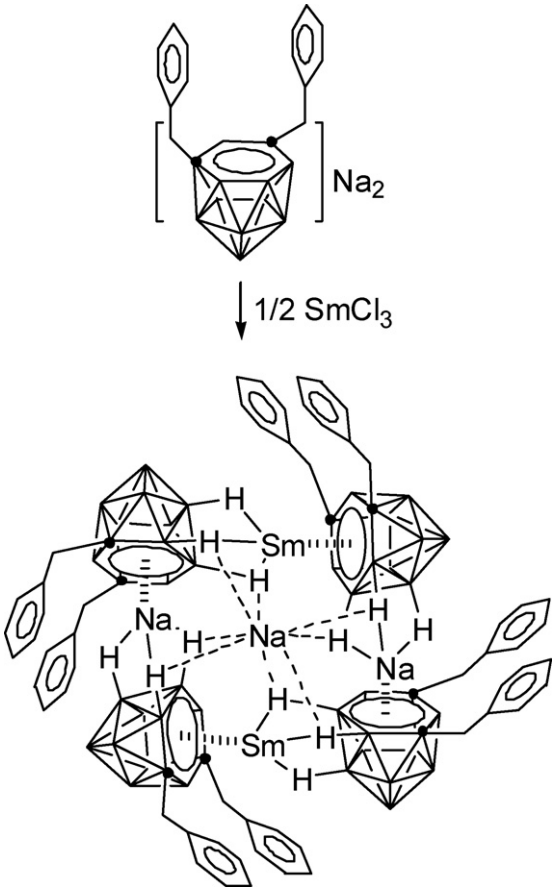

Scheme 26.

Sm(II) centers. An X-ray diffraction study reveals that this novel cluster consists of a central atom of sodium that bonds to four half-sandwich [1,6-$(PhCH_2)_2$-4,1,6-$MC_2B_{10}H_{10}$] (M = Na, Sm) units in a distorted-tetrahedral arrangement. The formation of Sm(II) is ascribed to the strong reducing power of the CAp *nido*-carborane anion [67].

Treatment of CAd salt [{7,8-[*o*-$C_6H_4(CH_2)_2$]-7,8-$C_2B_{10}H_{10}$}$_2$$Na_4(THF)_6]_n$ with 2 equiv. of $LnCl_3$ in THF generated the first examples of half-sandwich 13-vertex lanthanacarborane chlorides 4-Cl-4,4,4-$(THF)_3$-1,2-[*o*-$C_6H_4(CH_2)_2$]-4,1,2-$LnC_2B_{10}H_{10}$ (Ln = Nd, Er, Y) [68] (Scheme 27). The monomeric structure of the erbium complex was confirmed by X-ray diffraction. As shown in Fig. 16, the Er^{3+} ion is η^6-bound to the CAd *nido*-C_2B_{10} unit via a six-membered C_2B_4 bonding face, σ-bound to a terminal Cl atom and coordinated by three THF molecules in a distorted-square-pyramidal geometry. The average Er-cage atom and Er-Cl distances are 2.77(2) and 2.544(4) Å, respectively. The chloro group in these complexes can be substituted by other moieties, leading to the isolation of 4-[$(\mu$-$H)_3$BH]-4,4,4-$(THF)_3$-1,2-[*o*-$C_6H_4(CH_2)_2$]-4,1,2-$NdC_2B_{10}H_{10}$ and 4-(η^5-C_5H_5)-4-THF-1,2-[*o*-$C_6H_4(CH_2)_2$]-4,1,2-$YC_2B_{10}H_{10}$ [68] (Scheme 27). The replacement of a Cl^- by a Cp^- or BH_4^- does not lead to much change of the 13-vertex cage structure. A 13-vertex divalent ytterbacarborane [4,4,4-$(NC_5H_5)_3$-4-(μ-$Cl)_{0.5}$-1,2-[*o*-$C_6H_4(CH_2)_2$]-4,1,2-

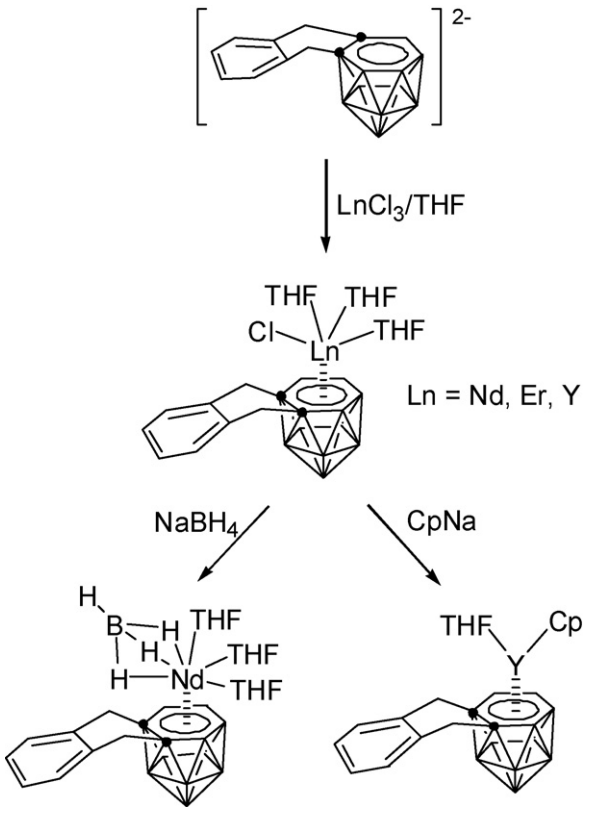

Scheme 27.

$YbC_2B_{10}H_{10}]_2[Na(NC_5H_5)_2]$ was prepared via the reaction of CAd [{7,8-[*o*-$C_6H_4(CH_2)_2$]-7,8-$C_2B_{10}H_{10}$}$_2$$Na_4(THF)_6]_n$ with $YbCl_3$ [68] (Scheme 28). The formation of this Yb(II) species indicates the reducing power of this CAd dianion. Such a redox reaction is also found in its reaction with $ZrCl_4$. As depicted in Scheme 29, two full-sandwich zirconacarboranes of the 4,1,2-type, {[*o*-$C_6H_4(CH_2)_2C_2B_{10}H_9]_2ZrCl_2$}{$Na(THF)_3$}$_2$ and {[*o*-$C_6H_4(CH_2)_2C_2B_{10}H_{10}]_2Zr$}{$Na(THF)_3$}$_2$, were isolated from the reaction mixture [69].

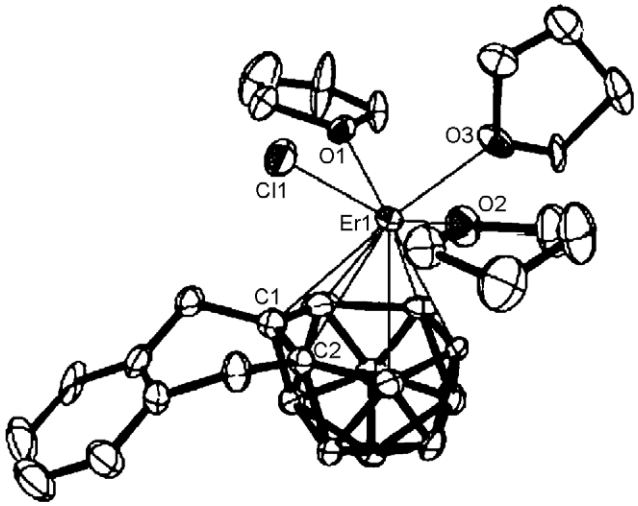

Fig. 16. Structure of {[*o*-$C_6H_4(CH_2)_2$]$C_2B_{10}H_{10}$}$ErCl(THF)_3$ reproduced by permission of The American Chemical Society from Ref. [68].

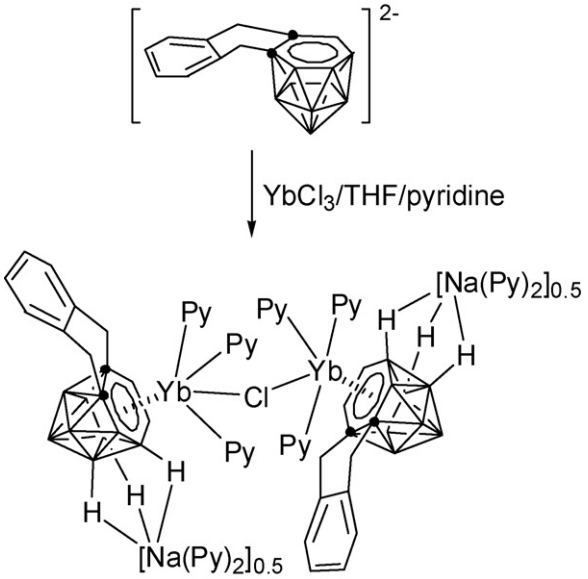

Scheme 28.

Attempts to prepare the mixed-sandwich lanthanacarborane $[(\eta^6\text{-}C_2B_{10}H_{12})(\eta^5\text{-}C_5Me_5)Eu(THF)_2]^-$ fail owing to the ligand redistribution which gives a homoleptic Eu complex $[(\eta^6\text{-}C_2B_{10}H_{12})_2Eu(THF)_2]^{2-}$ [66]. To prevent such a ligand redistribution reaction, the Xie group developed a family of linked carboranyl-cyclopentadienyl ligands [15]. Treatment of $LnCl_3$ with an equimolar amount of CAp $M_3[Me_2A(C_5H_4)(C_2B_{10}H_{11})]$ (M = Na, K; A = C, Si) in THF at room temperature gave the stable mixed-sandwich 13-vertex lanthanacarboranes $[\eta^5{:}\eta^6\text{-}Me_2A(C_5H_4)(C_2B_{10}H_{11})]Ln(THF)_2$ (Ln = Nd, Er; A = C, Si) of the 4,1,6-type, which were also prepared from the reaction of $[\eta^5\text{-}Me_2A(C_5H_4)(C_2B_{10}H_{11})]LnCl_2(THF)_3$ with 2 equiv. of K metal in THF [70,71] (Scheme 30). Under similar reaction conditions, however, interaction of $LnCl_3$ (Ln = Sm, Yb) with CAp $[Me_2Si(C_5H_4)(C_2B_{10}H_{11})]K_3$ in a molar ratio of 1:1 in THF did not afford the corresponding

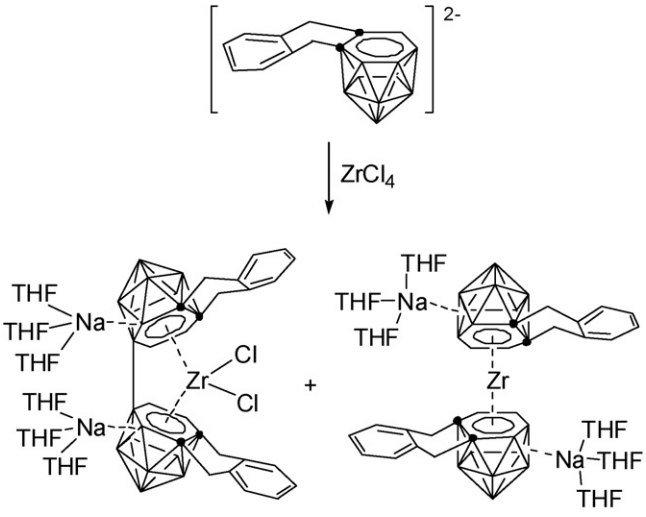

Scheme 29.

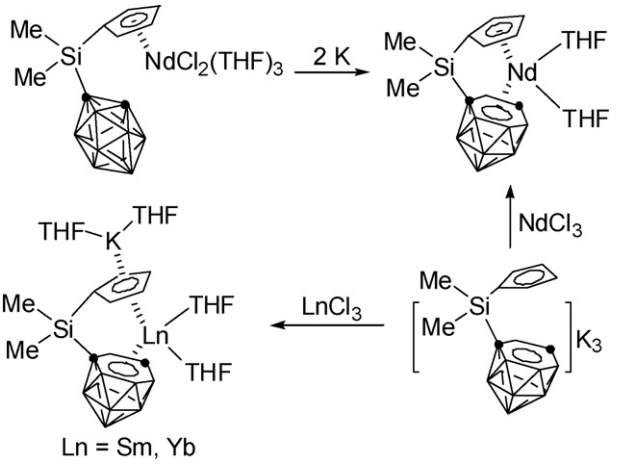

Scheme 30.

analogs. Instead, the 4,1,6-type of organolanthanide(II) species $\{[\eta^5{:}\eta^6\text{-}Me_2Si(C_5H_4)(C_2B_{10}H_{11})]Ln(THF)_2\}\{K(THF)_2\}$ (Ln = Sm, Yb) were isolated.

On the other hand, the 4,1,6-type of the trivalent samaracarborane $[\eta^5{:}\eta^6\text{-}Me_2Si(C_5H_4)(C_2B_{10}H_{11})]Sm(THF)_2$ was prepared by treatment of SmI_2 with 2 equiv. of $[Me_2Si(C_5H_4)(C_2B_{10}H_{11})]Na$ in THF [72] (Scheme 31). As revealed by single-crystal X-ray analyses, the Sm^{3+} ion is η^5-bound to the cyclopentadienyl ring, η^6-bound to the hexagonal C_2B_4 face of the cage and coordinated by two THF molecules in a distorted-tetrahedral geometry with a Cent–Sm–Cent angle of 125.1° (Fig. 17). The average Sm–cage atom and Sm–C(C_5 ring) distances are 2.803(3) and 2.706(2) Å, respectively. These results clearly indicate that the bridged ligand $[Me_2Si(C_5H_4)(C_2B_{10}H_{11})]^{3-}$ can indeed stabilize the mixed-sandwich lanthanacarboranes and effectively prevent the ligand redistribution reactions. The analogs $[\eta^5{:}\eta^6\text{-}Me_2C(C_5H_4)(C_2B_{10}H_{11})]Sm(THF)_2$ [73], $[\eta^5{:}\eta^6\text{-}Me_2Si(C_9H_6)(C_2B_{10}H_{11})]Sm(THF)_2$ [74], $[\{\eta^5{:}\eta^1{:}\eta^6\text{-}Me_2Si(C_9H_5CH_2CH_2OMe)(C_2B_{10}H_{10})Sm\}_2(\mu\text{-}$

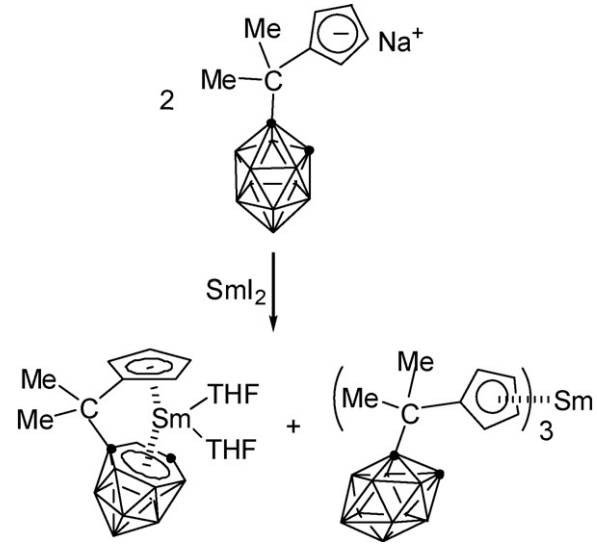

Scheme 31.

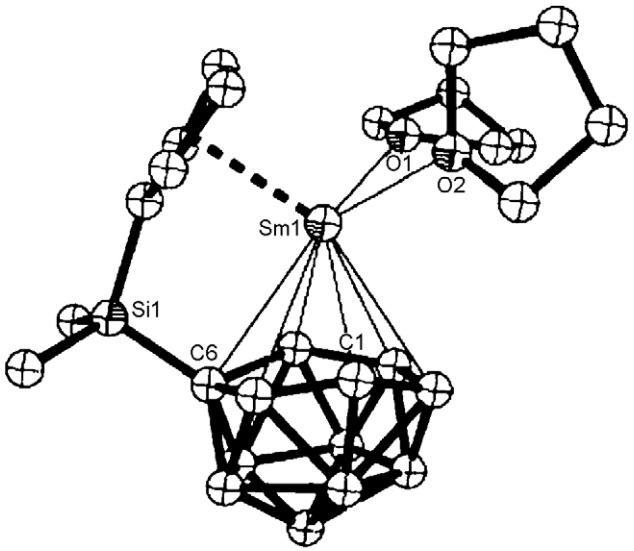

Fig. 17. Structure of $[\eta^5{:}\eta^6\text{-}Me_2Si(C_5H_4)(C_2B_{10}H_{11})]Sm(THF)_2$ reproduced by permission of The American Chemical Society from Ref. [72].

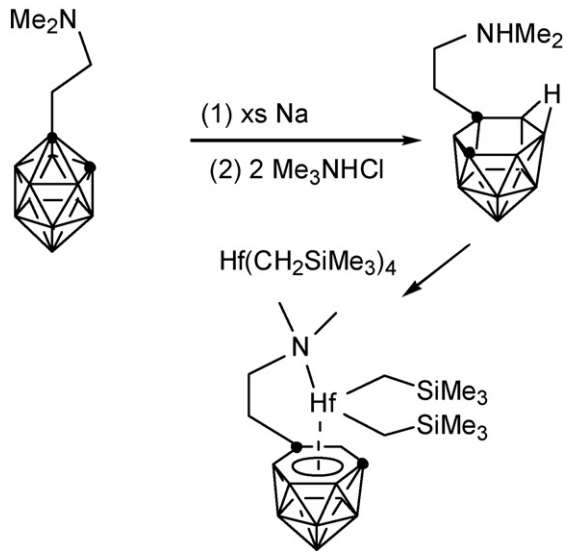

Scheme 33.

Cl)][Li(THF)$_4$] [75], and [{$\eta^5{:}\eta^1{:}\eta^6$-$Me_2Si(C_9H_5CH_2CH_2NMe_2)(C_2B_{10}H_{10})Sm$}$_2$($\mu$-Cl)][Li(THF)$_4$] [75] were also obtained in the same manner. Owing to the relatively lower reducing power of the Yb(II), the corresponding trivalent 13-vertex ytterbacarboranes cannot be prepared using such a redox method [72]. The formation of the above trivalent samaracarboranes may involve the reductive cage-opening followed by capitation. This process is also suggested for the formation of the 4,1,6-type of $[\eta^5{:}\eta^6{:}\sigma$-$Me_2Si(C_9H_6)(C_2B_{10}H_{10}CH_2NMe)]Zr(NC_5H_5)$ from the reaction of $[\eta^5{:}\sigma$-$Me_2Si(C_9H_6)(C_2B_{10}H_{10})]ZrCl(NMe_2)$ with ^{n}BuLi [76]. This species is a very rare example of high-valent 13-vertex group 4 metallacarboranes.

Recently, the Xie group developed a series of Lewis base appended carboranyl ligands and studies their applications in lanthanide and group 4 metal chemistry. Reaction of 1-$Me_2NCH_2CH_2$-1,2-$C_2B_{10}H_{11}$ with excess Na metal in THF, followed by treatment with 1 equiv. of YCl_3, afforded the 4,1,6-type of 13-vertex yttracarborane $[\sigma{:}\eta^6$-$(Me_2NCH_2CH_2)C_2B_{10}H_{11}]YCl(THF)_3$ containing a terminal Y–Cl bond (Scheme 32). Recrystallization from MeCN/toluene gave $[\sigma{:}\eta^6$-$(Me_2NCH_2CH_2)C_2B_{10}H_{11}]YCl(MeCN)_3$ [77]. Single-crystal X-ray analyses confirm that it is a monomeric half-sandwich complex in which the Y atom is η^6-bound to a hexagonal C_2B_4 bonding face, σ-bound to a terminal chloro ligand, and coordinated to the nitrogen atoms of the sidearm and three MeCN molecules in a highly distorted-octahedral geometry. Treatment of this chloro species with 1 equiv. of Cp″Li in THF gave $[\sigma{:}\eta^6$-$(Me_2NCH_2CH_2)C_2B_{10}H_{11}]YCp''(\mu$-Cl)Li(THF)$_2$ that was structurally characterized [77] (Scheme 32).

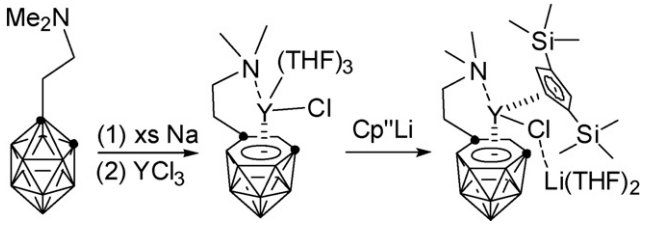

Scheme 32.

The first 13-vertex group 4 metallacarborane alkyl complex is very recently synthesized via alkane elimination method. Interaction between zwitterionic salt 7-$Me_2NHCH_2CH_2$-7,9-$C_2B_{10}H_{12}$ and $Hf(CH_2SiMe_3)_4$ gave a half-sandwich hafnacarborane alkyl $[\sigma{:}\eta^6$-$(Me_2NCH_2CH_2)C_2B_{10}H_{11}]Hf(CH_2SiMe_3)_2$ [78] (Scheme 33). This study opens new opportunities for the investigation of M–C σ bond in metallacarboranes. Single-crystal X-ray diffraction studies reveal that the Hf atom is η^6-bound to the open C_2B_4 bonding face of a *nido*-carboranyl ligand, σ-bound to two CH_2SiMe_3 units, and coordinated to the nitrogen atom of the sidearm in a three-legged piano-stool geometry, as shown in Fig. 18. The Hf–cage atom distances range from 2.489(4) to 2.732(5) Å with an average value of 2.602(5) Å, indicating a highly asymmetrical η^6-bonding.

The Hosmane group reported that treatment of the CAp $[Me_2Si(NR)(C_2B_{10}H_{11})]Na_3$ with an equimolar amount of MCl_4 in THF produced $[\eta^1{:}\eta^6$-$Me_2Si(NR)(C_2B_{10}H_{11})]MCl(THF)_n$ (M = Ti, $n = 0$; M = Zr, $n = 1$) [79] (Scheme 34). Their structures have not been subjected to X-ray analyses yet. The formation of the M(IV) complexes is very interesting since it has been documented that MCl_4 can be easily reduced by CAp $[nido\text{-}R_2C_2B_{10}H_{10}]^{2-}$ to give the divalent species [38]. It might be assumed that the presence of the M–N σ bond could stabilize the high oxidation state of the central metal ion.

3.1.1.2. MC_2B_{10} system bearing arachno-C_2B_{10} ligand. In 1999, the Xie group reported the synthesis and structural characterization of a novel uranacarborane complex $[\{(\eta^7$-$C_2B_{10}H_{12})(\eta^6$-$C_2B_{10}H_{12})U\}\{K_2(THF)_5\}]_2$ from the reaction of *o*-$C_2B_{10}H_{12}$ with excess K metal in THF in the pres-

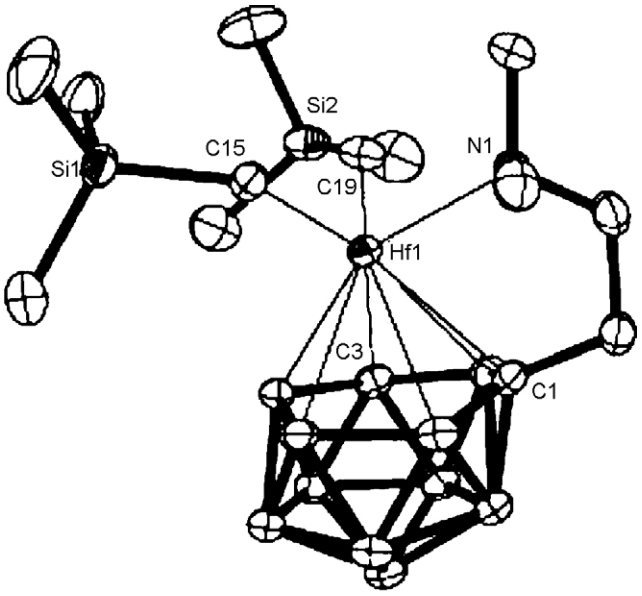

Fig. 18. Structure of $[\sigma{:}\eta^6\text{-}(Me_2NCH_2CH_2)C_2B_{10}H_{11}]Hf(CH_2SiMe_3)_2$ reproduced by permission of The American Chemical Society from Ref. [78].

ence of UCl_4 [80] (Scheme 35). This complex represents not only the first 13-vertex metallacarborane containing an *arachno* $[\eta^7\text{-}C_2B_{10}H_{12}]^{4-}$ ligand but also the first actinacarborane bearing a $[\eta^6\text{-}C_2B_{10}H_{12}]^{2-}$ ligand. As shown in Fig. 19, each U atom is η^6-bound to $[nido\text{-}C_2B_{10}H_{12}]^{2-}$, η^7-bound to $[arachno\text{-}C_2B_{10}H_{12}]^{4-}$, and coordinated to two B–H bonds from the C_2B_5 bonding face of the neighboring $[arachno\text{-}C_2B_{10}H_{12}]^{4-}$ ligand in a highly distorted-tetrahedral geometry with a Cent(C_2B_4)–U–Cent(C_2B_5) angle of 136.4°. It is not clear why the other $[nido\text{-}C_2B_{10}H_{11}]^{2-}$ dianion in this complex cannot be reduced to the $[arachno\text{-}C_2B_{10}H_{12}]^{4-}$ tetraanion in the presence of excess K metal. It may be speculated that this complex represents an intermediate going from $(\eta^6\text{-}C_2B_{10}H_{12})_2U$ to $(\eta^7\text{-}C_2B_{10}H_{12})_2U^{4-}$.

Interaction of $[\eta^5\text{-}Me_2C(C_5H_4)(C_2B_{10}H_{11})]LnCl_2(THF)_3$ or $[\eta^5{:}\eta^6\text{-}Me_2C(C_5H_4)(C_2B_{10}H_{11})]Ln(THF)_2$ with excess Na

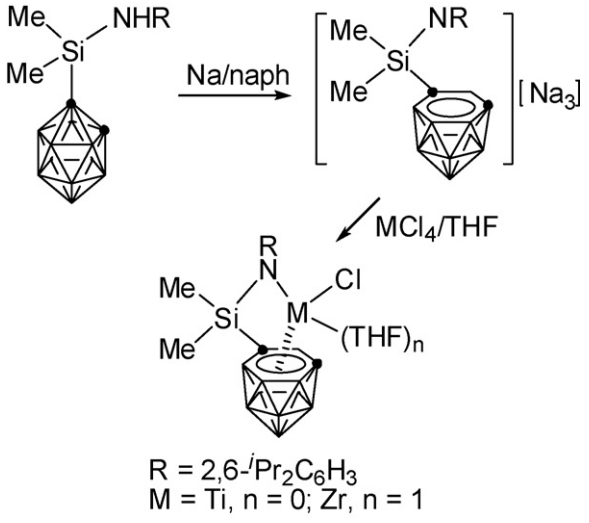

Scheme 34.

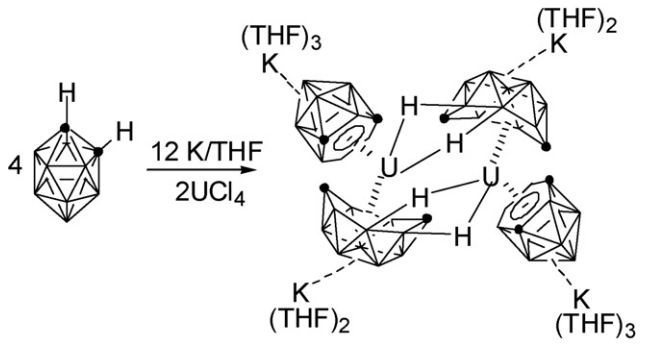

Scheme 35.

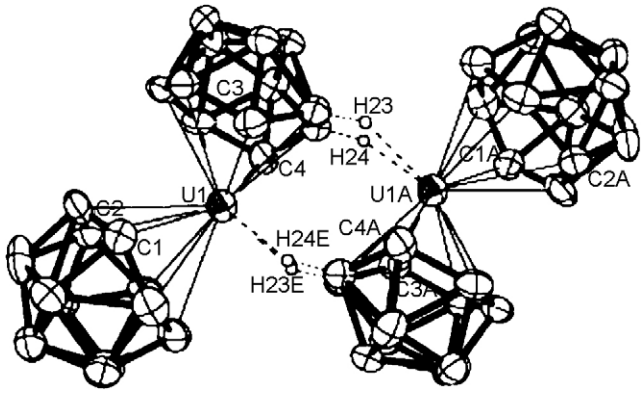

Fig. 19. Structure of $[\{(\eta^7\text{-}C_2B_{10}H_{12})(\eta^6\text{-}C_2B_{10}H_{12})U\}_2]^{4-}$ reproduced by permission of Wiley–VCH from Ref. [80].

metal in THF at room temperature afforded the same 13-vertex lanthanacarboranes bearing an *arachno*-η^7-carborane ligand, $[\{[\eta^5{:}\eta^7\text{-}Me_2C(C_5H_4)(C_2B_{10}H_{11})]Ln\}_2\{Na_4(THF)_9\}]_n$ (Ln = Dy, Er) [71,73] (Scheme 36). Their polymeric nature has been confirmed by an X-ray diffraction study. Each asymmetrical unit contains two 13-vertex $\{[\eta^5{:}\eta^7\text{-}Me_2C(C_5H_4)(C_2B_{10}H_{11})]Er\}^{2-}$ structural motifs that are connected to each other by three Na atoms through several B–H–Na bonding interactions. The carborane ligand $[arachno\text{-}C_2B_{10}H_{11}]^{4-}$ has a boat-like C_2B_5 bonding face in which the five B atoms are coplanar and the two C atoms are ca. 0.6 Å above this plane, resulting in an average Er–C(cage) distance being ca. 0.26 Å shorter than the average Er–B(cage)

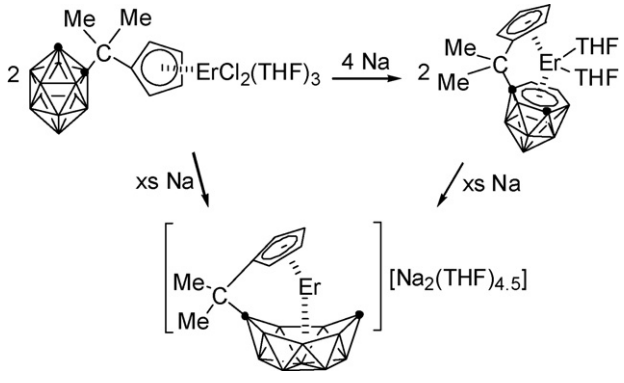

Scheme 36.

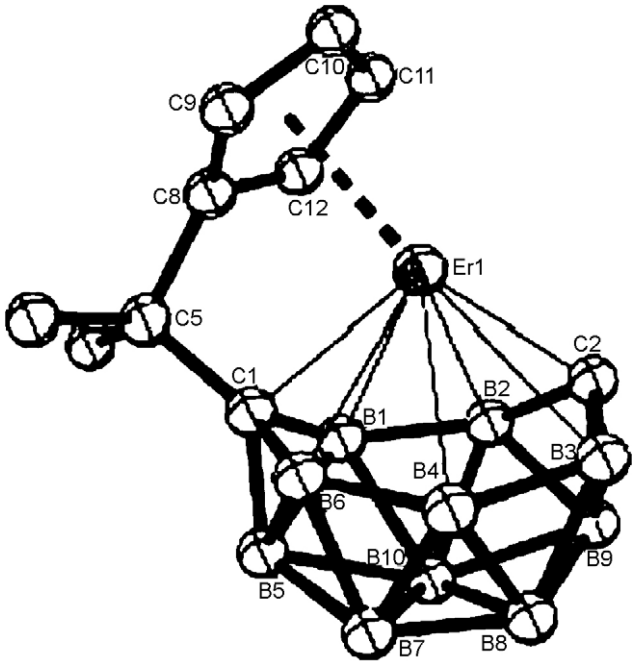

Fig. 20. Structure of $\{[\eta^5{:}\eta^7\text{-}Me_2C(C_5H_4)(C_2B_{10}H_{11})]Er\}^{2-}$ reproduced by permission of The American Chemical Society from Ref. [73].

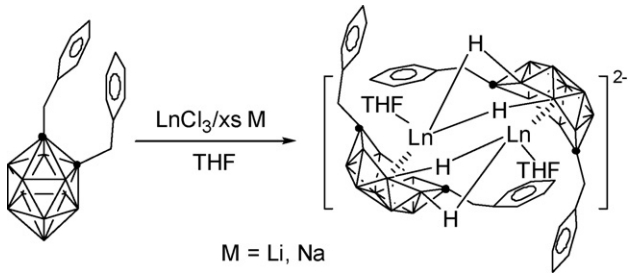

Scheme 37.

distance (Fig. 20). This is the first 13-vertex lanthanacarborane containing a η^7-carboranyl ligand.

Reduction of *o*-carborane derivatives 1,2-$(PhCH_2)_2$-1,2-$C_2B_{10}H_{10}$, 1-(XCH_2CH_2)-1,2-$C_2B_{10}H_{11}$, 1,2-$(XCH_2CH_2)_2$-1,2-$C_2B_{10}H_{10}$ (X = OMe, NMe_2), $Me_2Si(C_9H_7)(C_2B_{10}H_{11})$, $(ArCH_2)_2C_2B_{10}H_{10}$ (Ar = 3,5-$(CH_3O)_2C_6H_3$, 1-pyrenyl), and $(C_9H_7)C_2B_{10}H_{11}$ with group 1 metals in the presence of $LnCl_3$ gave the corresponding 13-vertex lanthanacarboranes in which the *arachno*-carboranyl ligands all bond to the Ln^{3+} in η^7-fashion [81–83] (Schemes 37 and 38). Since the *closo*-

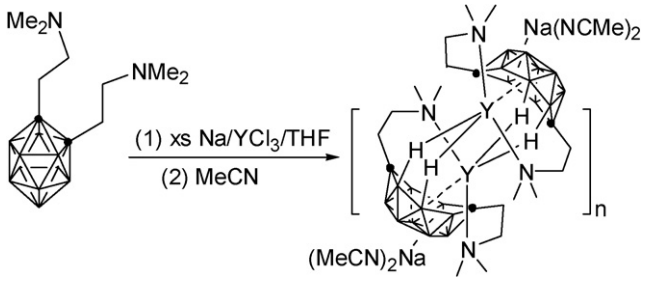

Scheme 38.

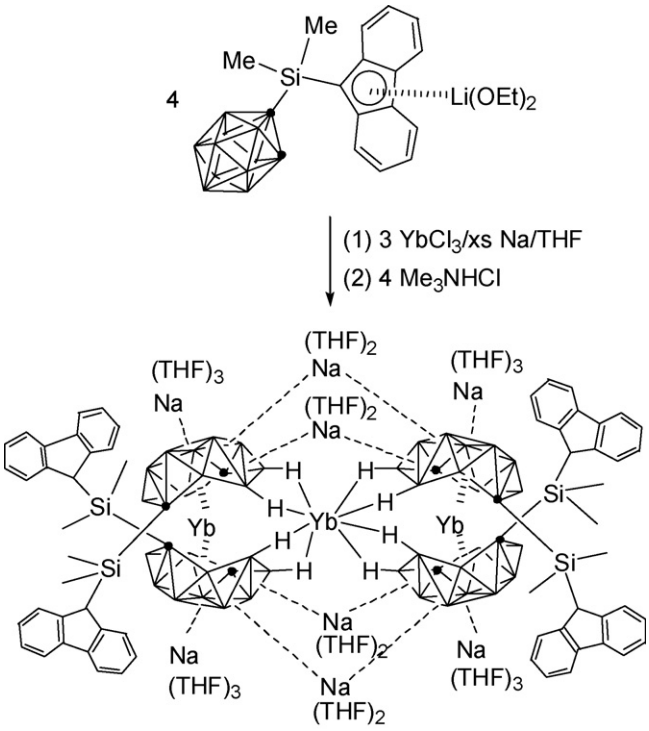

Scheme 39.

carboranes cannot be directly converted into the *arachno* tetraanions by group 1 metals, it is very reasonable to suggest that the 13-vertex metallacarboranes $[\eta^6\text{-}R_2C_2B_{10}H_{10}]LnCl(THF)_x$ may serve as intermediates which accept two more electrons from group 1 metals to form the final product.

The *arachno*-η^7-carborane tetraanions can effectively stabilize the high oxidation states of metal ions. Interaction between $YbCl_3$, 1 equiv. of $[Me_2Si(C_{13}H_8)(C_2B_{10}H_{11})]Li(OEt_2)_2$ and excess finely cut Na metal in THF at room temperature, followed by treatment with 1 equiv. of dry Me_3NHCl produced a novel full-sandwich lanthanacarborane $\{\{[\eta^7\text{-}Me_2Si(C_{13}H_9)(C_2B_{10}H_{11})]_2Yb^{III}\}_2Yb^{II}\}\{Na_8(THF)_{20}\}$ [84] (Scheme 39), in which the η^7-bonded ytterbium atoms retain their oxidation state +3 although excess sodium metal was used. This argument is supported by the isolation of 13-vertex high-valent group 4 metallacarboranes, $[\{(\mu{:}\eta^5){:}\eta^7\text{-}Me_2Si(C_5H_4)(C_2B_{10}H_{11})\}Zr(NEt_2)\{Na_3(THF)_4\}]_n$ [76], $[\eta^1{:}\eta^1{:}\eta^7\text{-}(Me_2NCH_2CH_2)(MeOCH_2CH_2)(C_2B_{10}H_{10})]Zr(\mu\text{-}Cl)Na(THF)_3$ [85], and $[\eta^1{:}\eta^1{:}\eta^7\text{-}(Me_2NCH_2CH_2)_2(C_2B_{10}H_{10})]Zr(\mu\text{-}Cl)Na(THF)_3$ [85].

The above results show that (1) the arrangement of the cage atoms in *arachno*-η^7-$R_2C_2B_{10}H_{10}^{4-}$ is the same regardless of the substituents on the cage carbon atoms and the nature of central metal ions, and (2) *arachno*-$[\eta^7\text{-}R_2C_2B_{10}H_{10}^{4-}]$ prefer metal ions with d^0/f^n electronic configurations. To understand these features, molecular orbital calculations at the B3LYP level of the density functional theory have been performed on the model complex $[(\eta^7\text{-}C_2B_{10}H_{12})Y(H_2O)]_2^{2-}$ [81]. Careful examination of the molecular orbitals obtained from the calculations indicates that the metal's five d orbitals of Y are all significantly involved in the metal-$[\eta^7\text{-}C_2B_{10}H_{12}]$ bonding

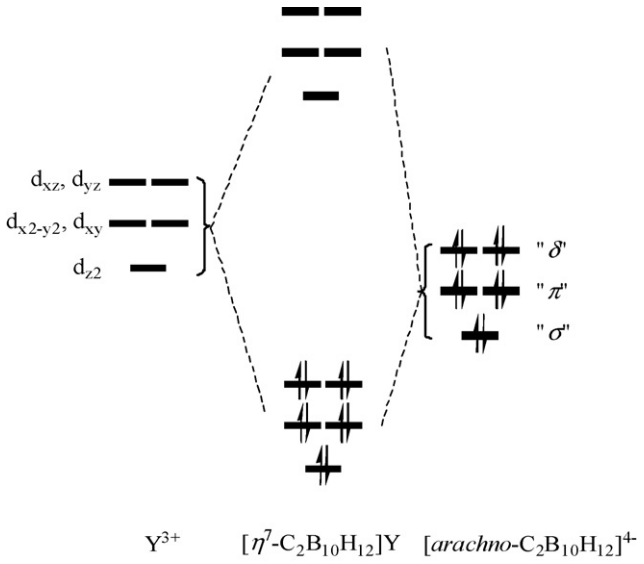

Fig. 21. Schematic orbital interaction diagram of Y^{3+} with $[arachno\text{-}\eta^7\text{-}C_2B_{10}H_{12}]^{4-}$ reproduced by permission of The American Chemical Society from Ref. [81].

interactions. The relevant molecular orbitals are mainly found in the HOMO-LUMO region. A schematic molecular orbital interaction diagram is shown in Fig. 21. The *arachno*-$[\eta^7\text{-}C_2B_{10}H_{12}]^{4-}$ moiety contributes five pairs of electrons to the five d orbitals of the metal ion to form metal-cage bond in η^7-fashion. It is anticipated that any d electrons of the central metal ion will destabilize the M-$[\eta^7\text{-}C_2B_{10}H_{12}]$ bonding interactions. These results explain why *arachno*-η^7-carboranyl ligand can stabilize the metal ions in their highest oxidation state, and only f-elements can form full-sandwich metallacarboranes with η^7-carboranyl ligands.

Another class of 13-vertex metallacarboranes containing *arachno*-C_2B_{10} ligands is derived from the CAd *arachno*-carborane tetraanions. As shown in Scheme 40, reduction of 4-Cl-4,4,4-$(THF)_3$-1,2-$[o\text{-}C_6H_4(CH_2)_2]$-4,1,2-$LnC_2B_{10}H_{10}$ with excess lithium or sodium metal gave the lanthanacarborane complexes $\{\eta^6\text{-}[1,2\text{-}[o\text{-}C_6H_4(CH_2)_2]\text{-}1,2\text{-}C_2B_{10}H_{10}]_2Ln\}^{5-}$ [68]. These species were also prepared by the direct interaction of the CAd *arachno*-$[\{1,2\text{-}[o\text{-}C_6H_4(CH_2)_2]\text{-}1,2\text{-}C_2B_{10}H_{10}\}Li_4(THF)_6]_2$ with $LnCl_3$. Fig. 22 shows the representative structure of a full-sandwich lanthanacarborane moiety $\{\eta^6\text{-}[\mu\text{-}1,2\text{-}[o\text{-}C_6H_4(CH_2)_2]\text{-}1,2\text{-}C_2B_{10}H_{10}]_2Er\}^{5-}$. The two hexagonal C_2B_4 bonding faces are not parallel to each other, but rather have a dihedral angle of 20.5°, and the Cent–Er–Cent angle is 152.1°.

3.1.2. MC_4B_8, $M_2C_3B_8$, $M_2C_2B_9$, and $M_3C_3B_7$ systems

A limited number of 13-vertex metallacarboranes of the types of MC_4B_8, $M_2C_3B_8$, $M_2C_2B_9$, and $M_3C_3B_7$ have been known. Insertion of metal cations into the $R_4C_4B_8H_8^{2-}$ anions afforded the MC_4B_8 type of complexes [86–91]. These capitation reactions are very complicated, generating a mixture of products, from which four 13-vertex species were isolated and structurally characterized, $(\eta^5\text{-}Me_4C_4B_8H_8)$Ni(dppe) [88], $(Et_4C_4B_8H_7)_2(COMe_2)_2CoH$

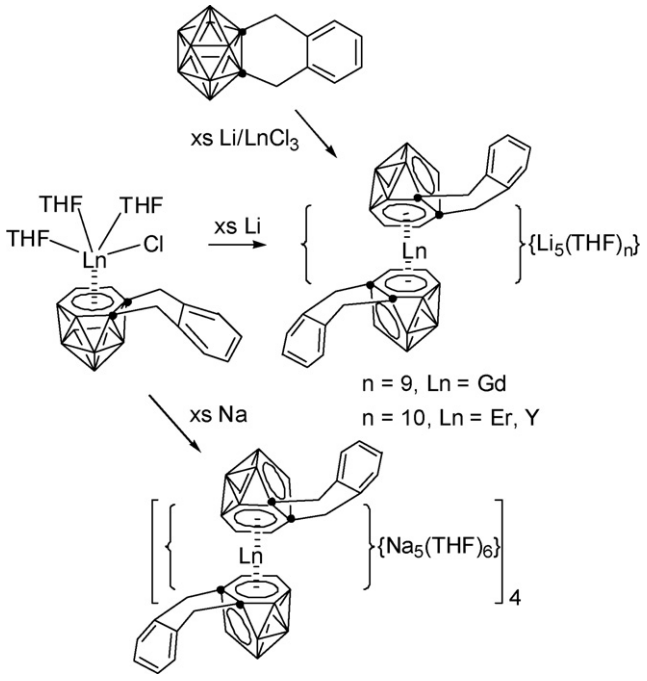

Scheme 40.

[90], $(Et_2C_2B_4H_4)Co(Et_4C_4B_8H_7OC_4H_8)$ [91], and $(\eta^6\text{-}Et_4C_4B_8H_8)Cr(\eta^5\text{-}Cp)$ [89]. Fig. 23 shows the molecular structure of $(\eta^5\text{-}Me_4C_4B_8H_8)$Ni(dppe) as a well-defined 13-vertex *nido* cage. Such an open cage geometry is also observed in other three complexes.

Bi- and trinuclear 13-vertex metallacarboranes are known. Reaction of 13-vertex cobaltacarborane 4-Cp-1,8-R_2-4,1,8-

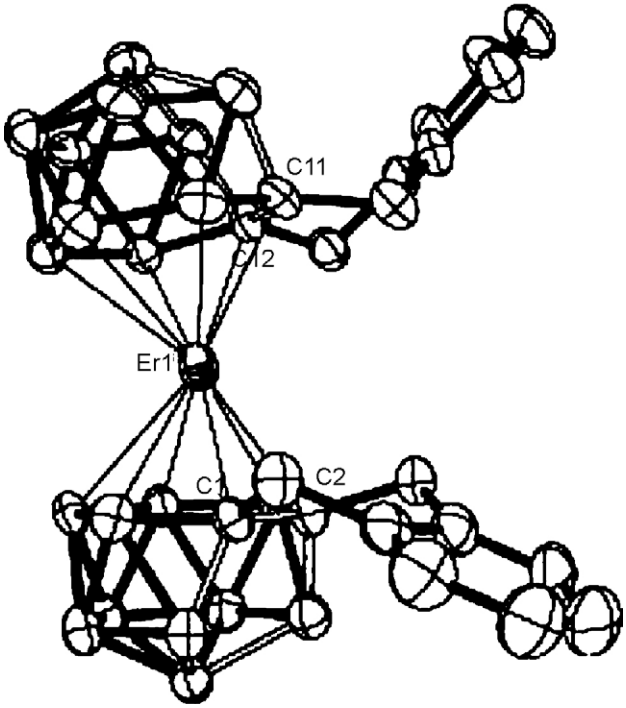

Fig. 22. Structure of $\{\eta^6\text{-}[1,2\text{-}[o\text{-}C_6H_4(CH_2)_2]\text{-}1,2\text{-}C_2B_{10}H_{10}]_2Er\}^{5-}$ reproduced by permission of The American Chemical Society from Ref. [68].

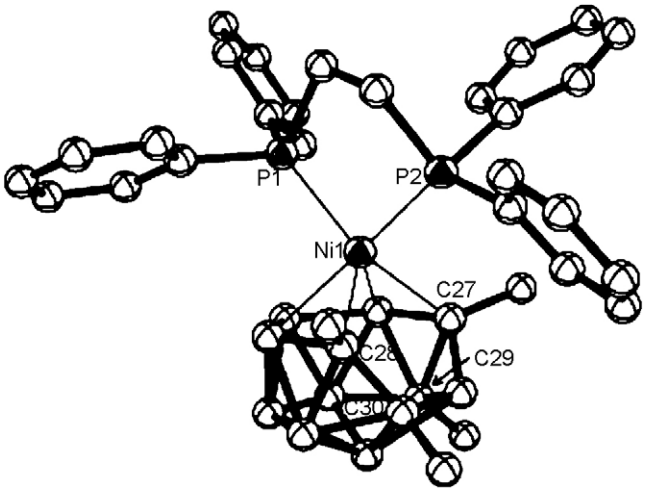

Fig. 23. Structure of (η^5-$Me_4C_4B_8H_8$)Ni(dppe) reproduced by permission of The American Chemical Society from Ref. [88].

$CoC_2B_{10}H_{10}$ or 4-Cp-1,12-R_2-4,1,12-$CoC_2B_{10}H_{10}$ with KOH in the presence of CpH and metal salt produced new 13-vertex bimetallacarborane 4,5-Cp_2-1,8-R_2-4,5,1,8-$CoMC_2B_9H_9$ or 4,5-Cp_2-1,12-R_2-4,5,1,12-$CoMC_2B_9H_9$ (M = Co, Fe), respectively. In the absence of CpH, a trinuclear complex $[NMe_4][(CpCoC_2B_9H_{11})_2Co]$ was obtained [92] (Scheme 41). These complexes are characterized by spectroscopic techniques, and their structures are postulated.

In 2002, the synthesis and structural characterization of the 13-vertex diruthenacarboranes of the $Ru_2C_2B_9$ type were reported [93]. Electrophilic insertion of $[Cp^*Ru]^+$ or $[CpRu]^+$ into the 12-vertex *closo*-$[Cp^*RuC_2B_9H_{11}]^-$ gave the 13-vertex species (η^5-Cp*)Ru(η^6:η^6-$C_2B_9H_{11}$)Ru(η^5-Cp*) or (η^5-Cp*)Ru(η^6:η^6-$C_2B_9H_{11}$)Ru(η^5-Cp), respectively, as shown in Scheme 42. The former was also prepared by the reaction of $Tl[TlC_2B_9H_{11}]$ with 0.5 equiv. of $[Cp^*RuCl]_4$. As shown in Fig. 24, (η^5-Cp*)Ru(η^6:η^6-$C_2B_9H_{11}$)Ru(η^5-Cp*) possesses

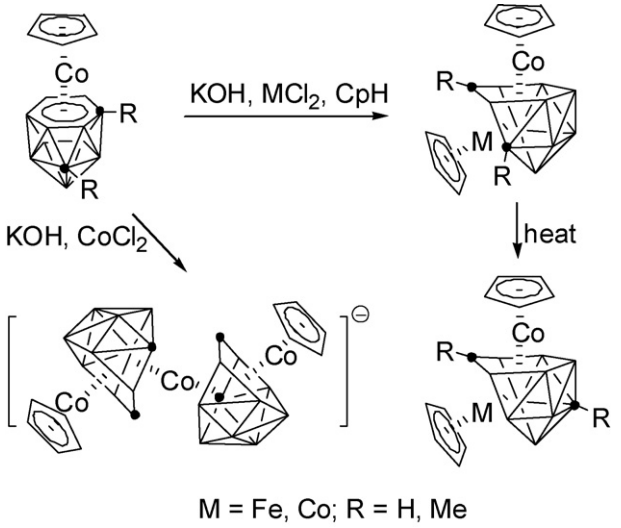

Scheme 41.

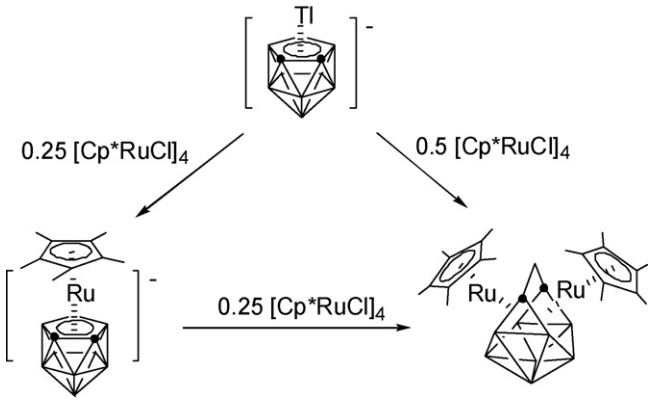

Scheme 42.

nearly ideal C_{2v} symmetry with the Ru and carbon vertices locating at the 4,5- and 2,3-positions, respectively, yielding a 4,5-Cp^*_2-4,5-Ru_2-2,3-$C_2B_9H_9$ structure. Each ruthenium atom is η^6-bound to the C_2B_4 faces with a common C_2B unit. There is no direct interaction between the two ruthenium atoms as demonstrated by the Ru(1)···Ru(2) distance of 3.531(1) Å. A similar complex $[Cp^*Ru(Me_2SC_2B_9H_{10})RuCp^*][Co(\eta^5\text{-}7,8\text{-}C_2B_9H_{11})_2]$ was obtained from the reaction of the zwitterion $Cp^*Ru(Me_2SC_2B_9H_{10})$ with a $[Cp^*Ru]^+$ source [94]. Although these 13-vertex cages are the violation of Wade's electron-counting rules as *isocloso* molecules [95], they show good thermal stabilities, which is attributed to the nearly nonbonding LUMOs as suggested for $[B_{13}H_{13}]^{2-}$ [93]. The parallel studies on the nickel, cobalt, and rhodium analogs do not produce the relevant 13-vertex species.

Cage reduction/metal insertion methodology is also used for the synthesis of 13-vertex diferracarboranes of the $Fe_2C_3B_8$ type [96]. Treatment of 2-Cp-9-^{t}BuNH-2,1,7,9-$FeC_3B_8H_{10}$ with $NaC_{10}H_8$ in DME produced presumably $[^t$BuNH-$CpFeC_3B_8H_{10}]^{2-}$, followed by reaction with $CpFe(CO)_2I$ or $[CpFe(CO)_2]_2$ to generate three diferratricarbaboranes, 4,5-Cp_2-4,5,1,6,7-$Fe_2C_3B_8H_{11}$, 4,5-Cp_2-4,5,1,7,12-$Fe_2C_3B_8H_{11}$, and 7-^{t}BuNH-4,5-Cp_2-4,5,1,7,12-$Fe_2C_3B_8H_{10}$ (Scheme 43). X-ray diffraction studies show that their structures are quite similar

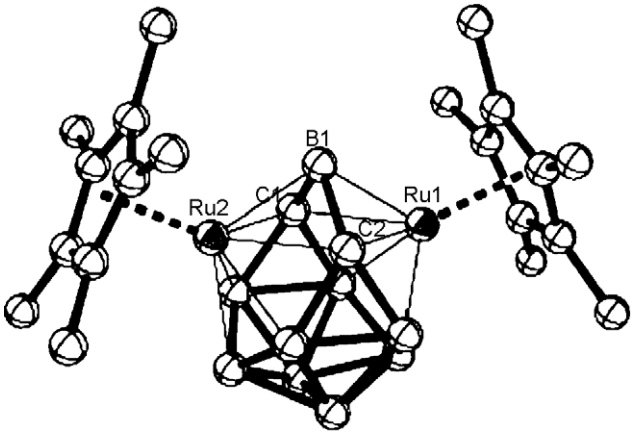

Fig. 24. Structure of (η^5-Cp*)Ru(η^6:η^6-$C_2B_9H_{11}$)Ru(η^5-Cp*) reproduced by permission of Wiley–VCH from Ref. [93].

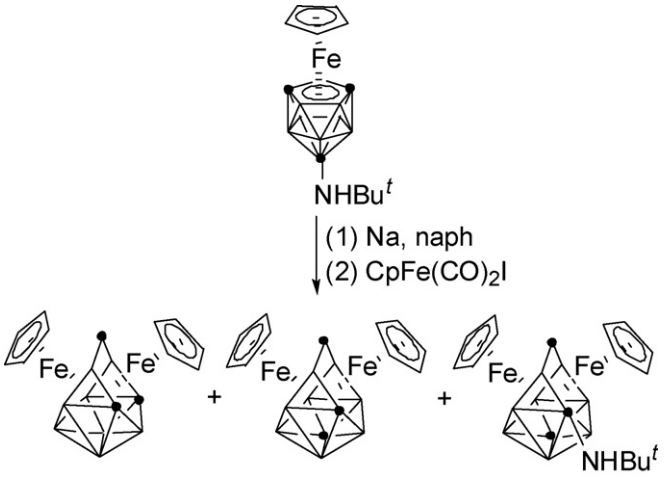

Scheme 43.

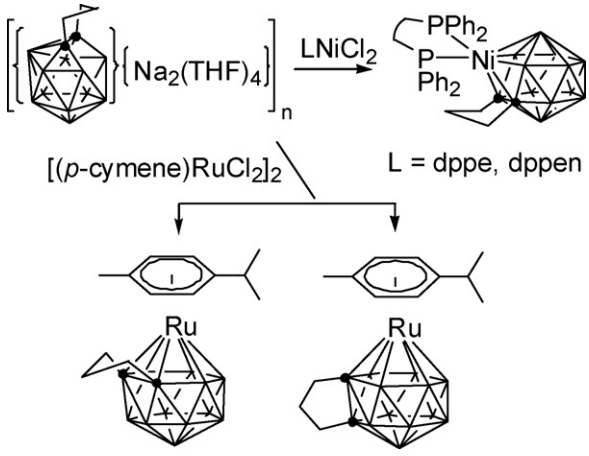

Scheme 44.

to that of the above mentioned diruthenium complex and both metal atoms occupy the 4,5-positions.

The only known trinuclear 13-vertex metallacarborane $Cp_2(Co_3C_3B_7H_{10})(C_2B_7H_9CH_2CH_2CN)$ was isolated from the reaction of *arachno*-6-$NCCH_2$-5,6,7-$C_3B_7H_{11}^-$ with $CoCl_2$ in the presence of CpNa [97]. X-ray analyses reveal that this species adopts a docosahedral geometry, in which the three Co atoms occupy three vertices with two being adjacent and are bonded to the carborane moiety in η^4-, η^4-, and η^6-fashion, respectively, as shown in Fig. 25.

3.2. Fourteen-vertex metallacarboranes

3.2.1. MC_2B_{11} system

Fourteen-vertex metallacarboranes of the MC_2B_{11} type are generally prepared from the 13-vertex *nido*-carborane anions. The Xie group reported that treatment of CAd *nido*-$[(CH_2)_3C_2B_{11}H_{11}]^{2-}$ with (L)$NiCl_2$ in THF gave 14-vertex nickelacarboranes (L)Ni[η^5-$(CH_2)_3C_2B_{11}H_{11}$] (L = dppe, dppen) [24] (Scheme 44). X-ray analyses reveal that they are isomorphous and isostructural. The geometry of the 14-vertex metallacarborane, Fig. 26, is a distorted-bicapped-hexagonal antiprism with two seven-coordinate boron vertices, which is similar to that of the 14-vertex carborane. Different from the 13-vertex metallacarboranes of the MC_2B_{10} system in which the metal is often bonded to the carborane cage in η^6 fashion,

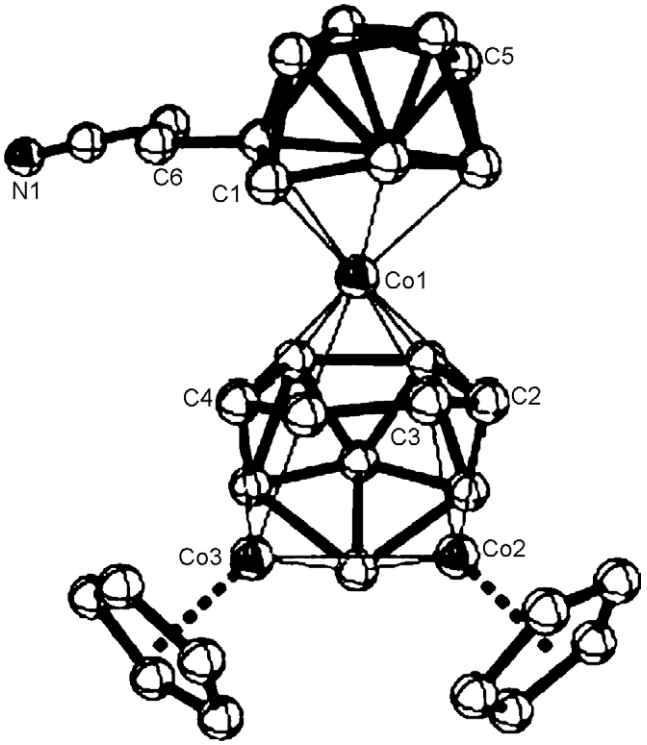

Fig. 25. Structure of $Cp_2(Co_3C_3B_7H_{10})(C_2B_7H_9CH_2CH_2CN)$ reproduced by permission of The American Chemical Society from Ref. [97].

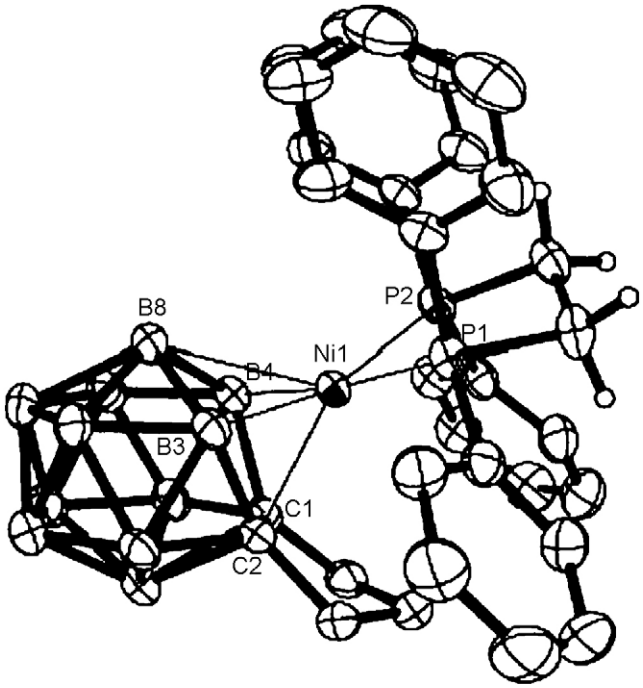

Fig. 26. Structure of 8-dppe-2,3-$(CH_2)_3$-8,2,3-$NiC_2B_{11}H_{11}$ reproduced by permission of The American Chemical Society from Ref. [24].

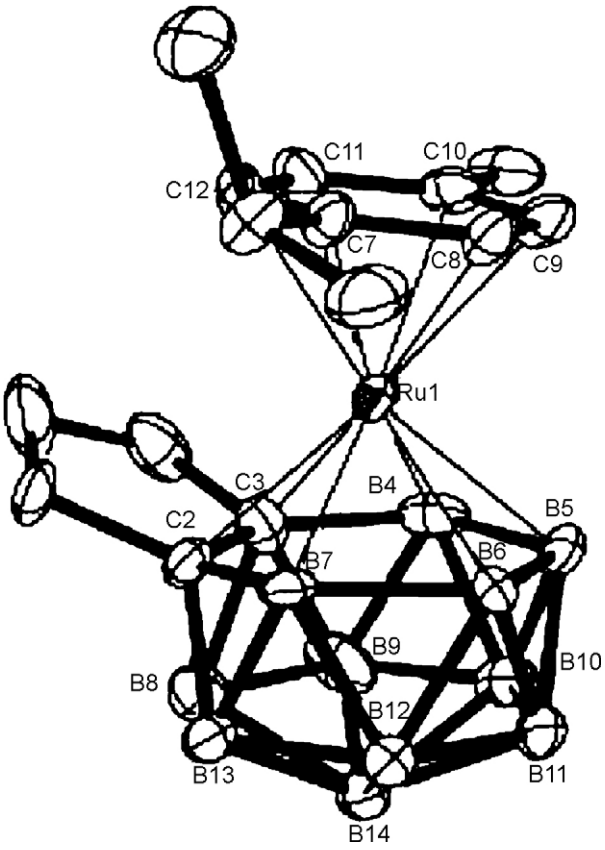

Fig. 27. Structure of 2,3-$(CH_2)_3$-1-(*p*-cymene)-1,2,3-$RuC_2B_{11}H_{11}$ reproduced by permission of Wiley–VCH from Ref. [25].

the Ni atom in the 14-vertex cages is bonded to the bent open face (C(1)C(2)B(3)B(4)B(8)) in η^5 fashion with a relatively long Ni(1)–B(8) bond distance of ~2.46 Å. Thus, these clusters may be viewed as 8-L-2,3-$(CH_2)_3$-8,2,3-$NiC_2B_{11}H_{11}$. The 14-vertex nickelacarboranes are much less stable than their 13-vertex analogs. Decomposition takes place when they are exposed to air and moisture, which might be due to the presence of longer Ni–B bonds in the cages.

Significantly different from the nickel species, the 14-vertex ruthenacarboranes 2,3-$(CH_2)_3$-1-(*p*-cymene)-1,2,3-$RuC_2B_{11}H_{11}$ and 2,8-$(CH_2)_3$-1-(*p*-cymene)-1,2,8-$RuC_2B_{11}H_{11}$, prepared from the reaction of CAd $Na_2[(CH_2)_3C_2B_{11}H_{11}]$ with $[(p\text{-cymene})RuCl_2]_2$, are quite air- and moisture-stable [25,26]. Single-crystal X-ray analyses reveal that they adopt bicapped hexagonal antiprism geometry, which is similar to that of the 14-vertex carboranes. The Ru atom occupies the 1-position and the two cage carbon atoms hold the 2,3- or 2,8-positions, respectively. Fig. 27 shows the molecular structure of the 1,2,3-isomer, in which the carboranyl is bonded to the ruthenium atom in η^6 fashion with the Ru–Cent(C_2B_4) distance of ~1.46 Å. Examination of the structures of the parent 13-vertex *nido*-carborane and 14-vertex ruthenacarboranes indicates that significant cage rearrangements occur during the reaction. The sizes of the central metal ions may play a role in this process. The proper selection of metal salts is crucial for the preparation of stable 14-vertex metallacarboranes [24]. For example, interaction of $SnCl_2$, $ZrCl_4$, or $(Ph_3P)_2PdCl_2$ with

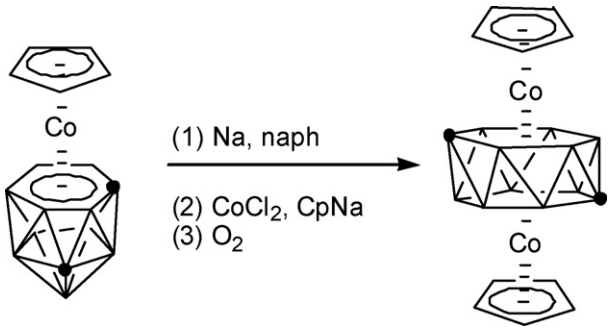

Scheme 45.

$Na_2[(CH_2)_3C_2B_{11}H_{11}]$ generated quantitatively 1,2-$(CH_2)_3$-1,2-$C_2B_{11}H_{11}$ according to the ^{11}B NMR analyses. In the cases of $(Ph_3P)_2NiCl_2$, $(Ph_3P)_2PtCl_2$, and $(Ph_3P)_3RuCl_2$, the reactions gave a mixture of inseparable products. These results suggest that the prevention of redox reactions is essential for the preparation of 14-vertex metallacarboranes.

3.2.2. $M_2C_2B_{10}$ system

Reduction of 13-vertex cobaltacarboranes 4-Cp-4,1,12-$CoC_2B_{10}H_{12}$ or 4-Cp-4,1,8-$CoC_2B_{10}H_{12}$ with 3 equiv. of sodium in the presence of naphthalene followed by the addition of CpNa and $CoCl_2$ gave, after air oxidation, the 14-vertex dinuclear metallacarboranes of the $M_2C_2B_{10}$ type, 1,14-Cp_2-1,14,2,10-$Co_2C_2B_{10}H_{12}$ and 1,14-Cp_2-l,14,2,9-$Co_2C_2B_{10}H_{12}$ [98] (Scheme 45). The molecular structures are proposed according to the NMR spectra. The cyclic voltammograms of these 14-vertex dicobaltacarboranes are similar to those of 13-vertex dicobaltacarboranes, showing reversible oxidative and reductive waves of a single electron redox process. In a similar manner, the following 14-vertex dinuclear metallacarboranes, 1-(*p*-cymene)-14-Cp-1,14,2,10-$RuCoC_2B_{10}H_{12}$, 1-(*p*-cymene)-14-(C_6H_6)-1,14,2,10-$Ru_2C_2B_{10}H_{12}$, 1,14-(*p*-cymene)$_2$-1,14,2,10-$Ru_2C_2B_{10}H_{12}$, and 1-(*p*-cymene)-14-(dppe)-1,14,2,10-$RuNiC_2B_{10}H_{12}$ were prepared by the Welch group [99] (Scheme 46). The structures of the latter two have been characterized by X-ray analyses, confirming their bicapped hexagonal antiprism geometries.

Fourteen-vertex dinuclear lithiacarboranes are also known. Treatment of 1,2-[*o*-$C_6H_4(CH_2)_2$]-1,2-$C_2B_{10}H_{10}$ with excess finely cut lithium metal in THF at room temperature produced, after workup, the first group 1 metal *arachno*-carborane tetraanionic salt $[\{\mu\text{-}1,2\text{-}[o\text{-}C_6H_4(CH_2)_2]\text{-}1,2\text{-}C_2B_{10}H_{10}\}Li_4(THF)_6]_2$. Other lithium salts of a general formula $[\{1,2\text{-}R_2\text{-}1,2\text{-}C_2B_{10}H_{10}\}Li_4(THF)_x]_2$ (R_2 = 1,8-$C_{10}H_6(CH_2)_2$, $(CH_2)_3$, $(CH_2)_4$, and $CH_2CH{=}CHCH_2$; $x = 5$ or 6) were also prepared in the same manner [100–102] (Scheme 47). As shown in Fig. 28, the *arachno*-carborane consists of one open six-membered C_2B_4 face and one open five-membered C_2B_3 face that are bonded to two lithium atoms in η^6- and η^5-fashion, respectively, to form a novel 14-vertex *closo*-dilithiacarborane. The average Li(1)–cage atom and Li(2)–cage atom distances of 2.315(8) and 2.309(10) Å are shorter than those observed in other lithiacarboranes [102].

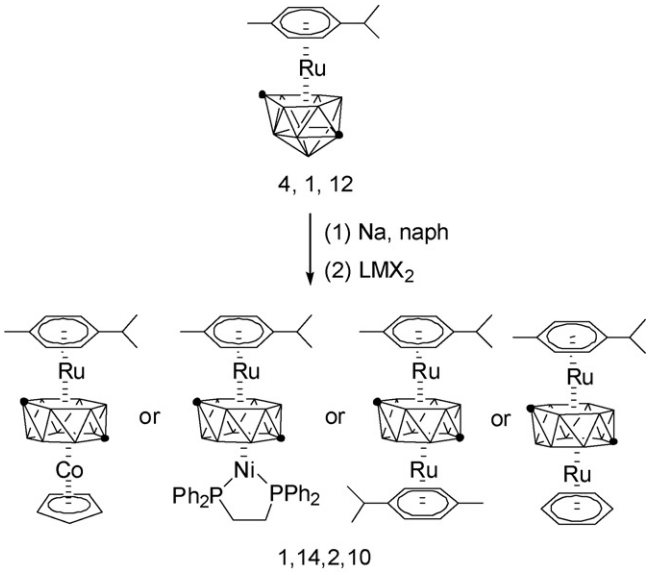

Scheme 46.

3.2.3. $M_2C_4B_8$ system

Reduction of $Me_4C_4B_8H_8$ with sodium in THF followed by treatment with $FeCl_2$ and CpNa offered four 14-vertex diferracarboranes of the general formula $Cp_2Fe_2Me_4C_4B_8H_8$ and a 12-vertex ferracarborane $CpFeMe_4C_4B_7H_8$ [86,103,104]. Scheme 48 shows the possible reaction pathway for the formation of 14-vertex species. Although all isomers contain 30 skeletal valence electrons, they have very different structures: three of them have irregular cage geometries with four- or five-membered open face, and the fourth one adopts a symmetrical structure of closed bicapped hexagonal antiprism.

3.3. Fifteen-vertex metallacarboranes

Very recently, the synthesis and structural characterization of two 15-vertex ruthenacarboranes are reported independently by two groups, which represent the largest metallacarboranes known to date. The Xie group reported that treatment of a 14-vertex *nido*-carborane salt $Na_2[(CH_2)3C_2B_{12}H_{12}]$ with $[(p\text{-cymene})RuCl_2]_2$ afforded a 15-vertex metallacarborane 1,4-$(CH_2)_3$-7-(*p*-cymene)-7,l,4-$RuC_2B_{12}H_{12}$ in 62% yield [25] (Scheme 49). An X-ray analysis reveals that its *closo* structure bears 26 triangulated faces and has an approximate D_{3h} symmetry, which is very similar to that predicted for $B_{15}H_{15}^{2-}$ by theoretical calculations (Fig. 29). Careful

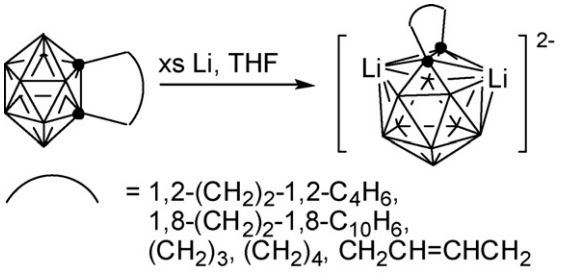

Scheme 47.

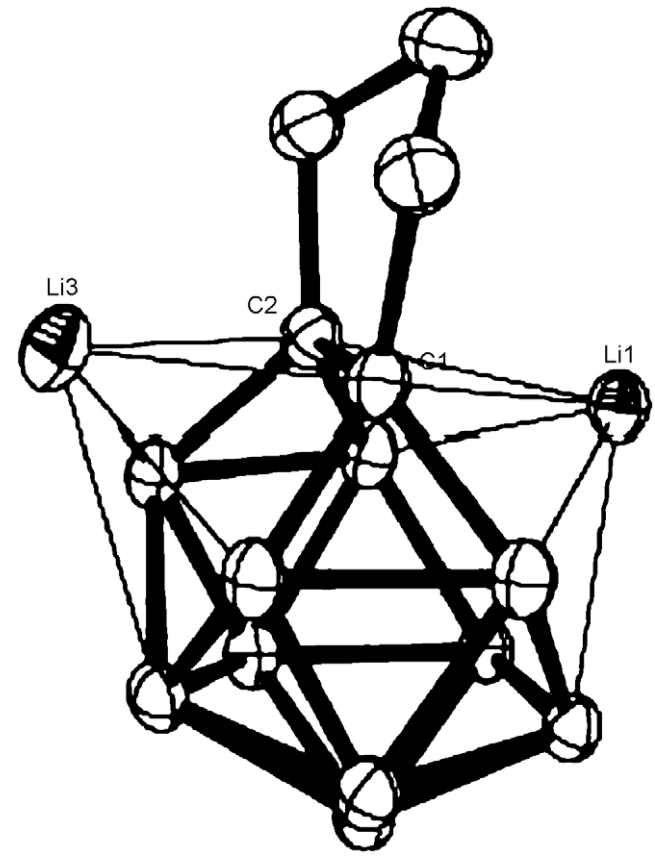

Fig. 28. Structure of $[2,3\text{-}(CH_2)_3\text{-}1,8,2,3\text{-}Li_2C_2B_{10}H_{10}]^{2-}$ reproduced by permission of The American Chemical Society from Ref. [101].

examination of the structures of the parent *nido* species and the 15-vertex metallacarborane clearly indicates that significant cage rearrangements occur during the reaction. On the other hand, the Welch group reported that 1,6-$(CH_2)_3$-7-(*p*-cymene)-7,1,6-$RuC_2B_{12}H_{12}$ was obtained upon thermolysis of the 14-vertex ruthenacarborane 2,8-$(CH_2)_3$-1-(*p*-cymene)-1,2,8-$RuC_2B_{11}H_{11}$ [26] (Scheme 50). The authors claim that the formation of this 15-vertex species should involve adventitious capture of a {BH} fragment. Direct reduction of the 14-vertex ruthenacarborane by Na metal followed by addition of RBX_2 does not give the 15-vertex metallacarboranes.

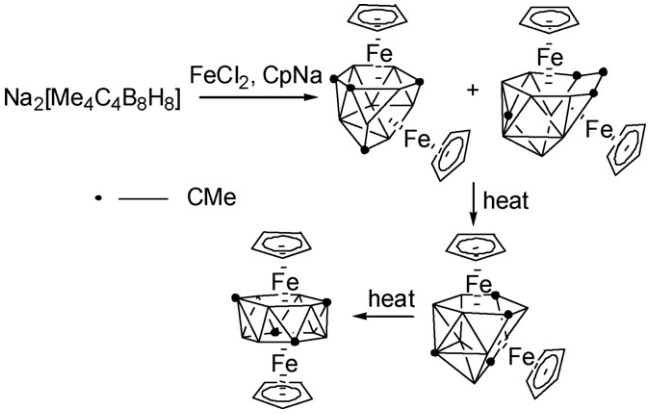

Scheme 48.

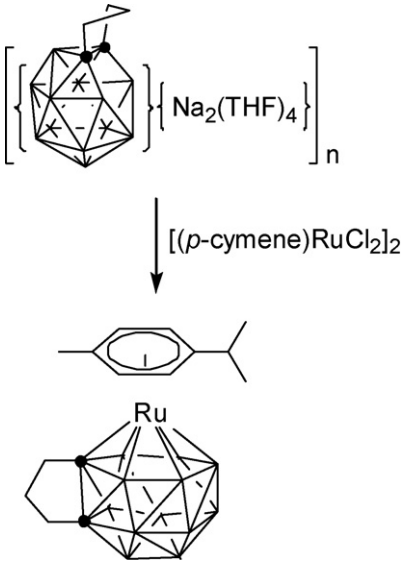

Scheme 49.

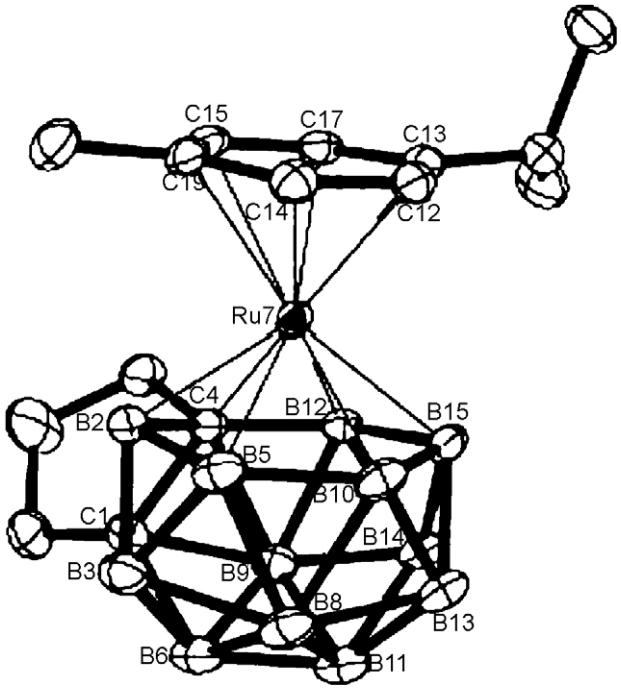

Fig. 29. Structure of 1,4-$(CH_2)_3$-7-(*p*-cymene)-7,l,4-$RuC_2B_{12}H_{12}$ reproduced by permission of Wiley–VCH from Ref. [25].

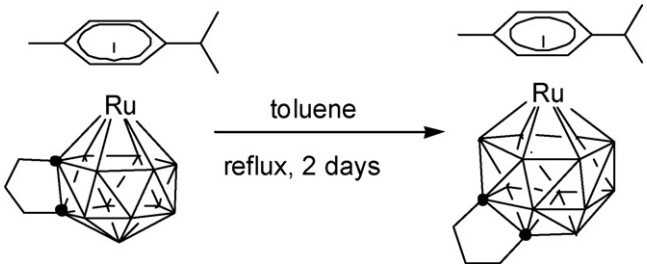

Scheme 50.

4. Conclusions and perspectives

Efforts of half a century in this research area have led to the extensive studies on the chemistry of carboranes and metallacarboranes. A large number of metallacarboranes with 13 vertices or more possessing very rich structural diversities have been prepared via different synthetic routes using various types of carboranyl ligands. The results show that both the carboranyl and ancillary ligands play an important role in the synthesis, structure, and reactivity of the resultant metallacarboranes. Since the cluster sizes of metallacarboranes are in principle controlled by those of carboranes, the successful syntheses of 13- and 14-vertex carboranes not only make the earlier predictions visible, but most importantly, lay a significantly new foundation to super-carborane and -metallacarborane chemistry.

Cage-opening and boron insertion method that work well for the preparation of 13- and 14-vertex carboranes have been unsuccessful when applied to the $(CH_2)_3C_2B_{12}H_{12}$ polyhedron owing to the redox reaction between the *nido*-$[(CH_2)_3C_2B_{12}H_{12}]^{2-}$ and RBX_2 reagents. New synthetic methodologies are desired for the production of larger clusters. A convergent $[12+n]$ approach ($n>2$) would be of great interest and full of challenges. As research in this area becomes more active, a new class of boron cluster of extraordinary size and unique structure would be envisioned. The search for applications of super-carboranes and -metallacarboranes in many disciplines such as BNCT, electronics, ceramics, catalysis, polymers and nanomaterials is anticipated in the future.

Acknowledgements

We thank The Research Grants Council of The Hong Kong Special Administration Region and The Chinese University of Hong Kong for financial support over the years. We are grateful to our collaborators with whom we have had the pleasure to interact.

Appendix A. Supplementary data

Supplementary data associated with this article can be found, in the online version, at doi:10.1016/j.ccr.2007.02.009.

References

[1] I. Shapiro, C.D. Good, R.E. Williams, J. Am. Chem. Soc. 84 (1962) 3837.
[2] M.F. Hawthorne, D.C. Young, P.A. Wegner, J. Am. Chem. Soc. 87 (1965) 1818.
[3] R.N. Grimes (Ed.), Carboranes, Academic Press, New York, 1970.
[4] T. Onak, in: E.W. Abel, F.G.A. Stone, G. Wilkinson (Eds.), Comprehensive Organometallic Chemistry II, vol. 1, Pergamon, New York, 1995, p. 217.
[5] R.N. Grimes, in: E.W. Abel, F.G.A. Stone, G. Wilkinson (Eds.), Comprehensive Organometallic Chemistry II, vol. 1, Pergamon, New York, 1995, p. 373.
[6] M. Davidson, A.K. Hughes, T.B. Marder, K. Wade, Contemporary Boron Chemistry, Royal Society of Chemistry, Cambridge, UK, 2000.
[7] Y.N. Bubnov, Boron Chemistry at the Beginning of the 21st Century, Russian Academy of Sciences, Moscow, Russia, 2002.
[8] Z. Xie, Coord. Chem. Rev. 250 (2006) 259.

[9] N.S. Hosmane, J.A. Maguire, Organometallics 24 (2005) 1356.
[10] I. Krossing, I. Raabe, Angew. Chem. Int. Ed. 43 (2004) 2066.
[11] N.S. Hosmane, J.A. Maguire, Eur. J. Inorg. Chem. 22 (2003) 3989.
[12] T.J. Wedge, M.F. Hawthorne, Coord. Chem. Rev. 240 (2003) 111.
[13] Z. Xie, Acc. Chem. Res. 36 (2003) 1.
[14] Z. Xie, Coord. Chem. Rev. 231 (2002) 23.
[15] J.F. Valliant, K.J. Guenther, A.S. King, P. Morel, P. Schaffer, O.O. Sogbein, K.A. Stephenson, Coord. Chem. Rev. 232 (2002) 173.
[16] R.N. Grimes, Coord. Chem. Rev. 200 (2000) 773.
[17] M.F. Hawthorne, A. Maderna, Chem. Rev. 99 (1999) 3421.
[18] A.H. Soloway, W. Tjarks, B.A. Barnum, F.-G. Rong, R.F. Barth, I.M. Codogni, J.G. Wilson, Chem. Rev. 98 (1998) 1515.
[19] A.K. Saxena, J.A. Maguire, N.S. Hosmane, Chem. Rev. 97 (1997) 2421.
[20] M.F. Hawthorne, Z.P. Zheng, Acc. Chem. Res. 30 (1997) 267.
[21] A.K. Saxena, N.S. Hosmane, Chem. Rev. 93 (1993) 1081.
[22] A. Burke, D. Ellis, B.T. Giles, B.E. Hodson, S.A. Macgregor, G.M. Rosair, A.J. Welch, Angew. Chem. Int. Ed. 42 (2003) 225.
[23] L. Deng, H.-S. Chan, Z. Xie, Angew. Chem. Int. Ed. 44 (2005) 2128.
[24] L. Deng, H.-S. Chan, Z. Xie, J. Am. Chem. Soc. 128 (2006) 5219.
[25] L. Deng, J. Zhang, H.-S. Chan, Z. Xie, Angew. Chem. Int. Ed. 45 (2006) 4309.
[26] R.D. McIntosh, D. Ellis, G.M. Rosair, A.J. Welch, Angew. Chem. Int. Ed. 45 (2006) 4313.
[27] L.D. Brown, W.N. Lipscomb, Inorg. Chem. 16 (1977) 2989.
[28] P.v.R. Schleyer, K. Najafian, A.M. Mebel, Inorg. Chem. 37 (1998) 6765.
[29] R.N. Grimes, Angew. Chem. Int. Ed. 42 (2003) 1198.
[30] A.S.F. Boyd, A. Burke, D. Ellis, D. Ferrer, B.T. Giles, M.A. Laguna, R. McIntosh, S.A. Macgregor, D.L. Ormsby, G.M. Rosair, F. Schmidt, N.M.M. Wilson, A.J. Welch, Pure Appl. Chem. 75 (2003) 1325.
[31] G. Zi, H.-W. Li, Z. Xie, Chem. Commun. (2001) 1110.
[32] G.B. Dunks, M.M. McKown, M.F. Hawthorne, J. Am. Chem. Soc. 93 (1971) 2541.
[33] M.R. Churchill, B.G. DeBoer, Chem. Commun. (1972) 1326.
[34] A. Burke, R. McIntosh, D. Ellis, G.M. Rosair, A.J. Welch, Collect. Czech. Chem. Commun. 67 (2002) 991.
[35] D.F. Dustin, G.B. Dunks, M.F. Hawthorne, J. Am. Chem. Soc. 95 (1973) 1109.
[36] C.G. Salentine, M.F. Hawthorne, J. Am. Chem. Soc. 97 (1975) 426.
[37] F.Y. Lo, C.E. Strouse, K.P. Callahan, C.B. Knobler, M.F. Hawthorne, J. Am. Chem. Soc. 97 (1975) 428.
[38] C.G. Salentine, M.F. Hawthorne, Inorg. Chem. 15 (1976) 2872.
[39] A. Burke, D. Ellis, D. Ferrer, D.L. Ormsby, G.M. Rosair, A.J. Welch, Dalton Trans. (2005) 1716.
[40] J.D. Hewes, C.B. Knobler, M.F. Hawthorne, Chem. Commun. (1981) 206.
[41] N.W. Alcock, J.G. Taylor, M.G.H. Wallbridge, J. Chem. Soc., Dalton Trans. (1987) 1805.
[42] G.K. Barker, M.P. Garcia, M. Green, F.G.A. Stone, A.J. Welch, Chem. Commun. (1983) 137.
[43] K.J. Donaghy, P.J. Carroll, L.G. Sneddon, J. Organomet. Chem. 550 (1998) 77.
[44] R. McIntosh, D. Ellis, J. Gil-Lostes, K.J. Dalby, G.M. Rosair, A.J. Welch, Dalton Trans. (2005) 1842.
[45] D. Ellis, M.E. Lopez, R. McIntosh, G.M. Rosair, A.J. Welch, R. Quenardelle, Chem. Commun. (2005) 1348.
[46] D.D. Devore, S.J.B. Henderson, J.A.K. Howard, F.G.A. Stone, J. Organomet. Chem. 358 (1988) C6.
[47] N. Carr, J.R. Fernandez, F.G.A. Stone, Organometallics 10 (1991) 2718.
[48] S.J. Crennell, D.D. Devore, S.J.B. Henderson, J.A.K. Howard, F.G.A. Stone, J. Chem. Soc., Dalton Trans. (1989) 1363.
[49] N. Carr, M.C. Gimeno, F.G.A. Stone, J. Chem. Soc., Dalton Trans. (1990) 2617.
[50] S.A. Brew, N. Carr, M.D. Mortimer, F.G.A. Stone, J. Chem. Soc., Dalton Trans. (1991) 811.
[51] S.A. Brew, N. Carr, J.C. Jeffery, M.U. Pilotti, F.G.A. Stone, J. Am. Chem. Soc. 114 (1992) 2203.
[52] N. Carr, D.F. Mullica, E.L. Sapperfield, F.G.A. Stone, Organometallics 12 (1993) 1131.
[53] S.J. Dossett, D.F. Mullica, E.L. Sappenfield, F.G.A. Stone, M.J. Went, J. Chem. Soc., Dalton Trans. (1993) 281.
[54] N. Carr, D.F. Mullica, E.L. Sappenfield, F.G.A. Stone, M.J. Went, Organometallics 12 (1993) 4350.
[55] S. Li, D.F. Mullica, E.L. Sappenfield, F.G.A. Stone, J. Organomet. Chem. 467 (1994) 95.
[56] M.A. Laguna, D. Ellis, G.M. Rosair, A.J. Welch, Inorg. Chim. Acta 347 (2003) 161.
[57] D.F. Mullica, E.L. Sappenfield, F.G.A. Stone, S.F. Woollam, Can. J. Chem. 73 (1995) 909.
[58] B.E. Hodson, T.D. McGrath, F.G.A. Stone, Dalton Trans. (2004) 2570.
[59] B.E. Hodson, T.D. McGrath, F.G.A. Stone, Organometallics 24 (2005) 3386.
[60] B.E. Hodson, T.D. McGrath, F.G.A. Stone, Organometallics 24 (2005) 1638.
[61] J.C. Jeffery, P.A. Jelliss, F.G.A. Stone, Inorg. Chem. 32 (1993) 3382.
[62] N.M.M. Wilson, D. Ellis, A.S.F. Boyd, B.T. Giles, S.A. Macgregor, G.M. Rosair, A.J. Welch, Chem. Commun. (2002) 464.
[63] K.-H. Wong, H.-S. Chan, Z. Xie, Organometallics 22 (2003) 1775.
[64] R. Khattar, C.B. Knobler, M.F. Hawthorne, J. Am. Chem. Soc. 112 (1990) 4962.
[65] R. Khattar, C.B. Knobler, M.F. Hawthorne, Inorg. Chem. 29 (1990) 2191.
[66] R. Khattar, M.J. Manning, C.B. Knobler, S.E. Johnson, M.F. Hawthorne, Inorg. Chem. 31 (1992) 268.
[67] Z. Xie, Z. Liu, Q. Yang, T.C.W. Mak, Organometallics 18 (1999) 3603.
[68] G. Zi, H.-W. Li, Z. Xie, Organometallics 21 (2002) 3464.
[69] W.-C. Kwong, H.-S. Chan, Y. Tang, Z. Xie, Organometallics 23 (2004) 3098.
[70] Z. Xie, S. Wang, Z. Zhou, T.C.W. Mak, Organometallics 18 (1999) 1641.
[71] Z. Xie, K. Chui, Q. Yang, T.C.W. Mak, Organometallics 18 (1999) 3947.
[72] Z. Xie, S. Wang, Z. Zhou, T.C.W. Mak, Organometallics 17 (1998) 1907.
[73] K. Chui, Q. Yang, T.C.W. Mak, Z. Xie, Organometallics 19 (2000) 1391.
[74] Z. Xie, S. Wang, Q. Yang, T.C.W. Mak, Organometallics 18 (1999) 2420.
[75] S. Wang, H.-W. Li, Z. Xie, Organometallics 20 (2001) 3624.
[76] Y. Wang, H. Wang, H.-W. Li, Z. Xie, Organometallics 21 (2002) 3311.
[77] M.-S. Cheung, H.-S. Chan, Z. Xie, Organometallics 24 (2005) 4207.
[78] M.-S. Cheung, H.-S. Chan, Z. Xie, Organometallics 24 (2005) 3037.
[79] J. Wang, Y. Zhu, S. Li, C. Zheng, J.A. Maguire, N.S. Hosmane, J. Organomet. Chem. 680 (2003) 173.
[80] Z. Xie, C.G. Yan, Q.C. Yang, T.C.W. Mak, Angew. Chem. Int. Ed. 38 (1999) 1761.
[81] K. Chui, Q. Yang, T.C.W. Mak, W.H. Lam, Z. Lin, Z. Xie, J. Am. Chem. Soc. 122 (2000) 5758.
[82] (a) M.-S. Cheung, H.-S. Chan, Z. Xie, Organometallics 23 (2004) 517;
(b) S. Wang, Y. Wang, M.-S. Cheung, H.-S. Chan, Z. Xie, Tetrahedron 59 (2003) 10373;
(c) H. Shen, H.-S. Chan, Z. Xie, Organometallics 25 (2006) 2617.
[83] M.-S. Cheung, H.-S. Chan, Z. Xie, Organometallics 23 (2005) 4468.
[84] S. Wang, H.-W. Li, Z. Xie, Organometallics 20 (2001) 3842.
[85] M.-S. Cheung, H.-S. Chan, S.W. Bi, Z.Y. Lin, Z. Xie, Organometallics 23 (2005) 4333.
[86] W.M. Maxwell, R.F. Bryan, R.N. Grimes, J. Am. Chem. Soc. 99 (1977) 4008.
[87] W.M. Maxwell, R.N. Grimes, Inorg. Chem. 18 (1979) 2174.
[88] R.N. Grimes, E. Sinn, J.R. Pipal, Inorg. Chem. 19 (1980) 2087.
[89] R.B. Maynard, Z.-T. Wang, E. Sinn, R.N. Grimes, Inorg. Chem. 22 (1983) 873.
[90] Z.-T. Wang, E. Sinn, R.N. Grimes, Inorg. Chem. 24 (1985) 826.
[91] Z.-T. Wang, E. Sinn, R.N. Grimes, Inorg. Chem. 24 (1985) 834.
[92] D.F. Dustin, M.F. Hawthorne, J. Am. Chem. Soc. 96 (1974) 3462.
[93] A.R. Kudinov, D.S. Perekalin, S.S. Rynin, K.A. Lyssenko, G.V. Grintselev-Knyazev, P.V. Petrovskii, Angew. Chem. Int. Ed. 41 (2002) 4112.
[94] A.R. Kudinov, M.I. Rybinskaya, D.S. Perekalin, V.I. Meshcheryakov, Y.A. Zhuravlev, P.V. Petrovskii, A.A. Korlyukov, D.G. Golovanov, K.A. Lyssenko, Izv. Akad. Nauk SSSR, Ser. Khim. (2004) 1879.
[95] R.B. King, Inorg. Chem. 38 (1999) 5151, and references therein.

[96] B. Gruner, B. Stibr, R. Kivekas, R. Sillanpaa, P. Stopka, F. Teixidor, C. Vinas, Chem. Eur. J. 9 (2003) 6115.
[97] B.A. Barnum, P.J. Carroll, L.G. Sneddon, Inorg. Chem. 36 (1997) 1327.
[98] W.J. Evans, M.F. Hawthorne, J. Chem. Soc., Chem. Commun. (1974) 38.
[99] D. Ellis, M.E. Lopez, R. McIntosh, G.M. Rosair, A.J. Welch, Chem. Commun. (2005) 1917.
[100] G. Zi, H.-W. Li, Z. Xie, Organometallics 20 (2001) 3836.
[101] G. Zi, H.-W. Li, Z. Xie, Organometallics 21 (2002) 5415.
[102] L. Deng, M.-S. Cheung, H.-S. Chan, Z. Xie, Organometallics 24 (2005) 6244.
[103] W.M. Maxwell, R.F. Bryan, R.N. Grimes, J. Am. Chem. Soc. 99 (1977) 4016.
[104] J.R. Pipal, R.N. Grimes, Inorg. Chem. 17 (1978) 6.